AD-A090 559 TEL-AVIV UNIV (ISRAEL) QUANTUM ELECTRONICS LAB F/G 20/5
A UNIFIED THEORY OF MAGNETIC BREMSSTRAHLUNG, ELECTROSTATIC BREM--ETC(U)
MAY 80 A GOVER, P SPRANGLE AFOSR-80-0073
UNCLASSIFIED TAU-1980/81 AFOSR-TR-80-0934 NL

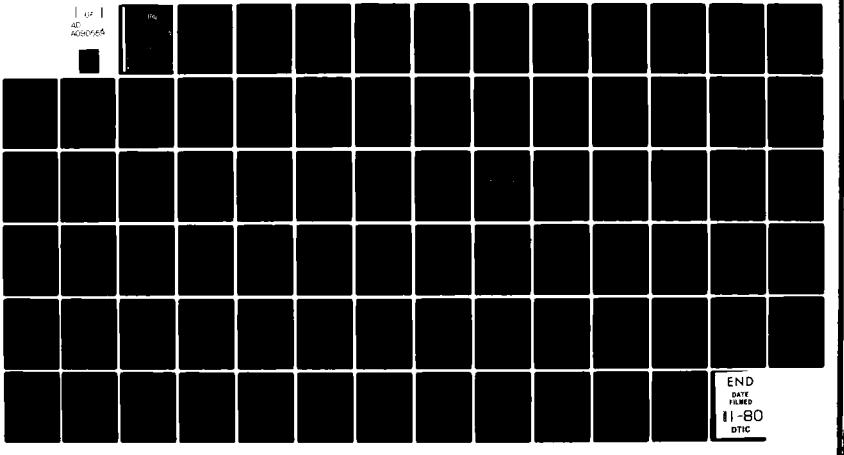

AD A090559

DDC FILE_COPY

LEVEL II

Interim rept. 1979-1980

DTIC

SEP 22 1980

411981

UNCLASSIFIED

SECURITY CLASSIFICATION OF THIS PAGE (When Data Entered)

REPORT DOCUMENTATION PAGE

READ INSTRUCTIONS BEFORE COMPLETING FORM

1. REPORT NUMBER: AFOSR-TR- 80-0934	2. GOVT ACCESSION NO.: AD-A090 559
	3. RECIPIENT'S CATALOG NUMBER:
4. TITLE (and Subtitle): A Unified Theory of Magnetic Bremsstrahlung, Electrostatic Bremsstrahlung, Compton-Raman Scattering and Cerenkov-Smith-Purcell Free Electron Lasers.	5. TYPE OF REPORT & PERIOD COVERED: Interim Scientific Report 1979/80
	6. PERFORMING ORG. REPORT NUMBER:
7. AUTHOR(s): A. Gover and P. Sprangle	8. CONTRACT OR GRANT NUMBER(s): AFOSR 80 - 0073
9. PERFORMING ORGANIZATION NAME AND ADDRESS: Tel-Aviv University, School of Engineering, Tel-Aviv, Israel.	10. PROGRAM ELEMENT, PROJECT, TASK AREA & WORK UNIT NUMBERS: 61102F, 2301/A1
11. CONTROLLING OFFICE NAME AND ADDRESS: Air Force Office of Scientific Research/NP, Bolling AFB, Washington DC. 20332	12. REPORT DATE: May 9, 1980
	13. NUMBER OF PAGES: 73
14. MONITORING AGENCY NAME & ADDRESS (if different from Controlling Office)	15. SECURITY CLASS. (of this report): unclassified
	15a. DECLASSIFICATION DOWNGRADING SCHEDULE

16. DISTRIBUTION STATEMENT (of this Report)

Approved for public release; distribution unlimited.

17. DISTRIBUTION STATEMENT (of the abstract entered in Block 20, if different from Report)

18. SUPPLEMENTARY NOTES

19. KEY WORDS (Continue on reverse side if necessary and identify by block number)

Free Electron Lasers, Cerenkov radiation, Smith-Purcell radiation, Bremsstrahlung, Compton scattering.

20. ABSTRACT (Continue on reverse side if necessary and identify by block number)

This article discusses in a comparative way the main operating parameters of various free electron lasers, providing a useful tool for laser design, and for comparative evaluation of the various lasers. We show that the various kinds of FELs satisfy the same gain-dispersion relation and differ only in a single coupling parameter κ. The different gain regimes which are common to all FELs are delineated. We find the small signal gain in all the gain regimes (warm and cold beam, low or high gain, single electron, collective or strong coupling

DD FORM 1473

UNCLASSIFIED

interaction). The laser gain parameter, radiation extraction efficiency, maximum power generation and spectral width are given and compared in the various kinds of FELs and gain regimes. The maximum power generation of all FELs (except Compton-Raman scattering) is shown to be limited by an interaction region width parameter. This parameter and consequently the laser power is larger in the highly relativistic limit by a factor $\sim\gamma_0$ in all bremsstrahlung FELs in comparison to Cerenkov-Smith-Purcell FELs. Some expressions which were derived earlier for the magnetic bremsstrahlung FEL, like the expression for gain in the low gain regime with space charge effect correction and the low gain expression for efficiency are shown to be special cases of more general expressions.

1. INTRODUCTION

We presently have a number of detailed theoretical analyses of free electron lasers (FEL) of various kinds: magnetic bremsstrahlung [1-10] electrostatic bremsstrahlung [11,13] stimulated Compton-Raman scattering [13-16] and Cerenkov-Smith-Purcell [17-21] However, it would be desirable at this point to have a simple unified model which describes simultaneously all the kinds of FELS, allowing easy comparison among the various lasers and providing simple expressions for the various operating parameters required for laser design.

As is shown in the next sections, such a unified analysis is possible because the different kinds of FELS all satisfy to a good approximation similar dispersion and gain relations. The origin of the similarity of the various FELs is that they all involve longitudinal coupling between single electrons or electron plasma waves and an electromagnetic wave. It is obviously so for the Cerenkov-Smith-Purcell FELS, but also in the magnetic bremsstrahlung FEL in which the electromagnetic wave has a transverse field only, and the electron beam is primarilytransversely modulated by the static magnetic field, there is a longitudinal interaction between the electromagnetic wave and the electron beam plasma, carried out through the ponderomotive potential (radiation pressure) [10].

The qualitative distinction among the different kinds of FEL mechanisms was discussed in detail in Ref. [17]. The basic difference between bremsstrahlung FELS and Cerenkov-Smith-Purcell FELS is that in the first case a periodic

(magnetostatic or electrostatic) force operates on the plasma waves, allowing phase matching (synchronism) with the electromagnetic wave by providing to the plasma waves negative crystal momentum $-k_o$:

$$k_o \equiv \frac{2\pi}{L} \tag{1}$$

where L is the periodicity of the periodic field. On the other hand, in the Cerenkov-Smith-Purcell FELs the synchronism is obtained by increasing the momentum (wave number) of the electromagnetic wave in a slow wave structure (a periodic waveguide or a dielectric waveguide).

The stimulated Compton Raman scattering problem is very similar to that of the bremsstrahlung FEL, except that instead of a static periodic force, the electron beam is modulated by an intense electromagnetic (pump) wave which propagates in a counter direction to the electron beam, and facilitates coupling between the electron plasma waves and a forward going scattered wave of higher frequency. The bremsstrahlung FEL is sometimes regarded as a special case of Compton-Raman scattering with zero frequency pump.

Fig.1 illustrates schematically the general structure of all the FELs discussed in the present article. They are all composed of an electron beam of uniform cross section which propagates at an average velocity v_{oz} through an electromagnetic waveguide and parallel to its axis (z direction). The crossed areas symbolically represent the source of interaction agent (pump) which allows the interaction between the electromagnetic wave and the electron plasma. This can be in different FELs coil windings, periodic magnets, periodic electrodes, a helix, corrugated walls, dielectric walls etc. The

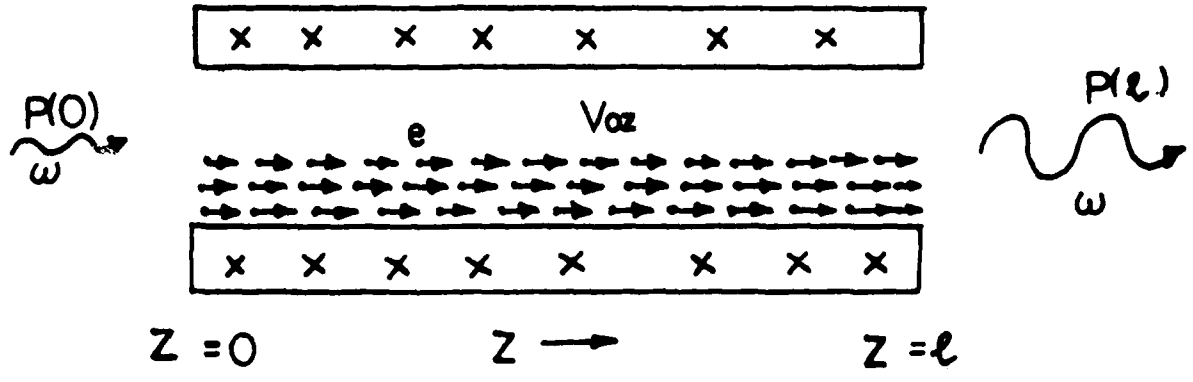

Fig. 1: A schematic representation of all kinds of FEL amplifier structures.

figure shows a schematical laser amplifier structure in which the input radiative power P(o) is amplified along an interaction length ℓ, producing an output power $P(\ell) > P(o)$. A free electron laser oscilator structure will consist of similar elements but will need in addition also means for a feedback mechanism (for example a Fabri-Perot resonator).

In the next section the radiation condition (wavelength of radiation) is derive for all FELs. In section 3 the common dispersion-gain relation of FELs is discussed. The different gain regimes, which evolve from the dispersion relation (and apply to all FELs) are delineated in section 4. Expressions for the maximum gain, efficiency, power and spectral width of the various FELS are derived in sections 5 to 8 and discussed in a comparative way.

Along the whole article we kept a full relativistic analysis. In most of the recent work on FELs the electron beam is highly relativistic. Therefore we gave the extreme relativistic limits of the relevant expressions (given in brackets). But in some FEL structures like the Smith-Purcell experiment [22], the Orotron [23,24] the Ledatron [25] or the Ubitron [26], the electron beam is non-relativistic or moderately relativistic. For this reason the derivation was made for all FELs (except stimulated Compton-Raman scattering) in a general way without using the somewhat simplifying assumption that the beam is highly relativistic.

The system of units used in this article is M.K.S.

2. THE RADIATION CONDITION

The radiation condition of the various free electron lasers can be derived from the kinematics of the interaction scheme, without requiring involved analysis.

In all FEL structures, shown schematically in Fig.1, an electron beam propagates inside the FEL structure together with a waveguided electromagnetic wave along the same direction (z axis). A necessary condition for interaction is close synchronism (phase matching)between the interacting electromagnetic wave and electron (plasma) waves. When such "near synchronism" is obtained, energy can be transferred from the electron beam to the radiation field (amplification) or vice versa (electron acceleration). This "synchronism" condition results in the radiation relation which determines the wavelengths at which amplification should be expected.

Fig.2 describes schematically the interaction schemes of the various free electron lasers discussed. The approximate wave numbers of the interacting waves or wave components (space harmonics) are listed in the first two columns of Table 1. Equating the wave numbers (phase matching or momentum conservation) yields the radiation condition (third column in Table 1). The expressions in brackets correspond to the highly relativistic limit $\gamma_{oz} >> 1$ (γ_{oz} is defined later in Eq. 7).

TABLE 1: The wavenumbers of the synchronous components of the interacting waves and the radiation condition for various FELS

FEL	EM Component wavenumber	Plasma Component wavenumber	Radiation Condition
Cerenkov	k_{zo}	$\frac{\omega}{v_o}$	$n^{-1}(\lambda)=\beta_o\cos\phi$
Smith Pur.	$k_{zo}+k_o$	$\frac{\omega}{v_o}$	$\frac{\lambda}{L} \simeq \beta_o^{-1}-\cos\phi$
Long.Brem.	k_{zo}	$\frac{\omega}{v_o} - k_o$	$\frac{\lambda}{L} \simeq \beta_o^{-1} -\cos\phi$
Trans.Brem.	k_{zo}	$\frac{\omega}{v_{oz}} - k_o$	$\frac{\lambda}{L} \simeq \beta_{oz}^{-1} -1= \frac{1}{(1+\beta_{oz})\beta_{oz}\gamma_{oz}^2} [\simeq \frac{1}{2\gamma_{oz}^2}]$
Compton-Raman	k	$\frac{\omega-\omega_o}{v_{oz}} - k_o$	$\frac{\lambda}{\lambda_o} = \frac{1}{(1+\beta_{oz})^2\gamma_{oz}^2} [\simeq \frac{1}{4\gamma_{oz}^2}]$

In Table 1 and Fig. 1 k_{zo} represents the wave number of the interacting electromagnetic wave which can be in general a waveguided mode for which $k_{zo}<k\equiv\omega/c$. Only for a plane wave propagating in the z direction, or alternatively a low order mode in a wide waveguide, one has $k_{zo} = k = \omega/c$. v_o is the mean velocity of the electron beam which is propagating in the z direction. In the case of the transverse pump FELs (two last rows in Table 1) the electron beam has at each point also transverse velocity and the parameter which is used in the synchronism condition is v_{oz} the longitudinal component of the average beam velocity. For the longitudinal FELs (first three rows in Table 1) $v_{oz} = v_o$ ($\gamma_{oz} = \gamma_o$).

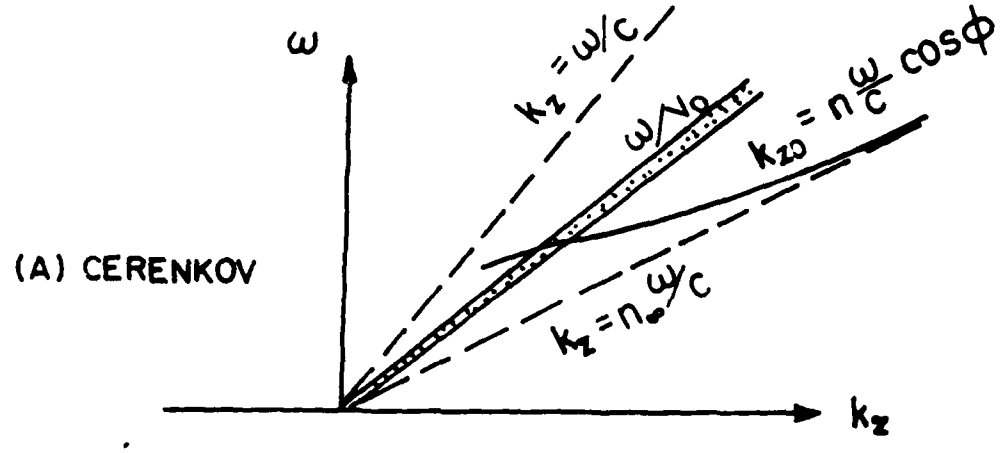

(A) CERENKOV

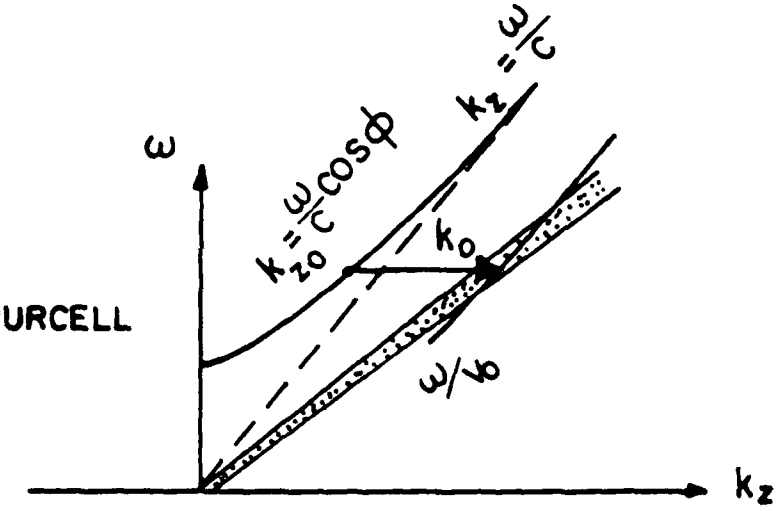

(B) SMITH – PURCELL

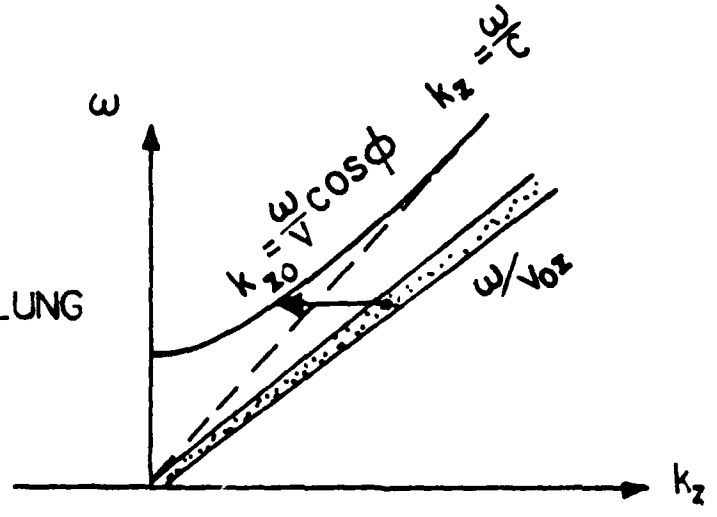

(C) BREMSSTRAHLUNG

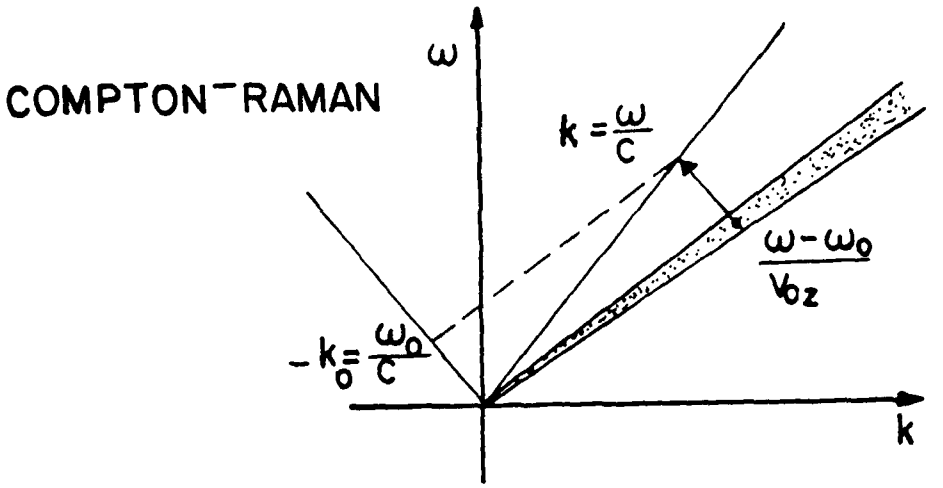

Fig. 2: Dispersion diagrams of the interacting waves illustrating the synchronism (phase matching) condition for the different FEL schemes.

The dispersion curve of the electron waves is represented symbolically in Fig.1 by the thick line of slope $\frac{\omega}{k_z} = v_{oz}$. A single electron which is forced to oscillate at frequency ω and at the same time propagates in the z direction with velocity v_z is generating a travelling current wave with wave number ω/v_z. In the case of a warm electron beam there is some spread in the wave numbers ω/v_z due to the variance v_{zth} in the velocities. When the beam is cold enough the eigenmodes of the beam plasma will be the longitudinal space charge waves with wave number $(\omega \pm \omega_p')/v_{oz}$. where ω_p' is the modified plasma frequency of the electron beam. Either case is represented approximately by the thick dotted line of slope v_{oz} assuming $v_{zth} << v_{oz}$ and $\omega_p' << \omega$.

The dispersion curve of the electromagnetic wave is in the case of Cerenkov FEL (Fig.2a) the well known dispersion curve of a dielectric waveguide mode which at high enough frequency tends to a slope (phase velocity) c/n (n is the high frequency index of refraction). If the beam which is propagated in close proximity to the dielectric waveguide, has a mean velocity $v_{oz} > c/n$, then synchronism between the electron beam and an electromagnetic mode may be possible around the curves crossing region:

$$\frac{\omega}{v_{oz}} > k_{zo} \qquad (2)$$

This can also be interpreted as a condition for synchronism between the wave phase velocity and the beam velocity $\omega/k_{zo} > v_{oz}$. The Radiation condition in Table 1 is derived from (2) using the definition of the "mode zig-zag angle"

$$\cos\theta < \frac{k_{zo}}{n(\omega)k} \qquad (3)$$

where $k \equiv \omega/c$.

In the case of the Smith Purcell FEL (Fig.1b) the synchronism (phase matching) between the electron beam waves and the electromagnetic mode is obtained by adding "crystal momentum k_o" to the mode wave number k_{z_o}. To be more concrete we may say that in the periodic waveguide, of which the Smith Purcell FEL is composed, the electromagnetic eigenmodes are Floquet-Bloch modes and the smooth waveguide dispersion diagram is modified into a Brillouin diagram with period k_o.(which for clarity is only partly drawn). The synchronism condition is obtained when the dispersion curve of the first order space harmonic $(k_{zo}+k_o)$ matches the curve of the electron beam wave:

$$\frac{\omega}{v_{oz}} \simeq k_{zo} + k_o \qquad (4)$$

This can also be interpreted as synchronism between the wave phase velocity and the beam velocity: $\omega/(k_{zo}+k_o) \simeq v_{oz}$. The radiation condition of the Smith Purcell effect [22] is derived in Table 1 from (4) using the definition for the "mode zig-zag angle"ϕ:

$$\cos\phi \equiv \frac{k_{zo}}{k} \qquad (5)$$

The scheme for the bremsstrahlung FEL (Fig.1c) is similar to that of the Smith-Purcell FEL and results the same synchronizm condition (4) and consequently the same radiation condition (Table 1). The difference is that in this case a periodic magnetic or electric force operates on the electron beam and endows its waves with a negative crystal momentum $-k_o$. Thus the electromagnetic waveguide mode interacts with the -1 order space harmonic of the electron

beam wave.

In the case of the most familiar transverse bremsstrahlung FEL (magnetic or electric), the interaction can take place with a transverse electromagnetic (TE) wave for which $k_{zo}=k$ ($\phi=0$). Hence the radiation condition for this case which is given in Table 1 (row 4) is derived by simply substituting $\phi=0$ in the previous result (row 3). In this case and also in the transverse electrostatic and Compton-Raman FELs the electron beam has a transverse component of the average beam velocity due to the transverse force applied by the pump, and $v_{oz}\neq v_o$. We defined for these cases

$$\beta_{oz} \equiv \frac{v_{oz}}{c} \tag{6}$$

$$\gamma_{oz} = (1-\beta_{oz}^2)^{-\frac{1}{2}} \tag{7}$$

In the first three rows of table 1 the FELs listed have only longitudinal interaction and the beam has no average transverse velocity. We substituted there $v_{oz} = v_o$.

In the case of Compton-Raman scattering (Fig.1d) the periodic electrostatic or magnetostatic pump of the transverse bremsstrahlung FEL is replaced by an intense TEM wave with frequency ω_o and wavenumber $k_o = 2\pi/\lambda_o$) propagating in a counter direction to the electron beam. The combined effect of the scattering and scattered electromagnetic waves generates in

the beam an electron current wave which oscillates with the difference frequency $\omega-\omega_o$ and propagates with wave number $(\omega-\omega_o)/v_{oz}-k_o$. The synchronism condition is

$$\frac{\omega-\omega_o}{v_{oz}} - k_o \simeq k \tag{8}$$

which results the radiation condition of Table 1 (row 5).

This synchronism condition can be also explained in a different way. The combined effect of the scattering and scattered waves generates in a parametric process a current with frequency $\omega-\omega_o$ and wave number $k+k_o$. The scattering process is resonant when the phase velocity of the current is synchronous with the electron beam

$$\frac{\omega-\omega_o}{k+k_o} \simeq v_{oz} \tag{9}$$

This is of course equivalent to (8).

3. THE DISPERSION-GAIN RELATION

We consider the interaction between an electromagnetic waveguide mode

$$\underline{E}(x,y,z) = a(o)\underline{\mathcal{E}}(x,y,z)e^{ik_{zo}z} \tag{10}$$

and an electron beam, both propagating in the +z direction in a free electron laser structure as shown in Fig.1. The waveguide can be either a uniform or a periodic waveguide.

Due to the interaction of the electromagnetic wave with the electron beam, its amplitude grows gradually at a spatial growth rate assumed to be small compared to a wavelength. With this assumption, and an assumption that only one mode exists in the waveguide, the Maxwell equations may be reduced into two simple one dimensional equations for the amplitude of the electromagnetic mode:[27,20,21]]

$$\frac{da(z)}{dz} - ik_{zo}a(z) = \frac{1}{4P}\int_{-\infty}^{\infty}\int_{-\infty}^{\infty}\underline{J}(x,y,z)\cdot\underline{\mathcal{E}}^{*}(x,y,z)\,dxdy \tag{11}$$

$$E_z(x,y,z) = a(z)\,\mathcal{E}_z(x,y,z) + \frac{1}{i\omega\varepsilon}\,J_z(x,y,z) \tag{12}$$

where a(z), the amplitude of the electromagnetic mode is defined by

$$\underline{E}_t(x,y,z) = a(z)\;\underline{\mathcal{E}}_t(x,y,z) \tag{13}$$

$\underline{\mathcal{E}}_t(x,y,z)$ is the transverse field component of the uncoupled electromagnetic mode (Eq.10), P is the Poynting vector power of this uncoupled mode

$$P \equiv \frac{1}{2}\int_{-\infty}^{\infty}\int_{-\infty}^{\infty}\mathrm{Re}\,[\underline{\mathcal{E}}_t(x,y,z)\times\underline{\tilde{\mathcal{H}}}_t(x,y,z)]\cdot i_z\,dxdy \tag{14}$$

This formalism is useful for most kinds of waveguides of relevance to free electron laser structures, including periodic waveguides. In the particular case of a uniform cross section waveguide (which is of relevance for all FELs except Smith-Purcell type) the uncoupled mode field is independent of z: $\underline{\mathcal{E}}(x,y,z) = \underline{\mathcal{E}}(x,y)$. In the Smith-Purcell FEL $\underline{\mathcal{E}}(x,y,z)$ is a periodic function of z with the period of the periodic waveguide-L.

The current $\underline{J}(x,y,z)$ is the alternating current which is induced in the electron beam by the interaction mechanism of any kind of free electron laser scheme. When $\underline{J}=o$ (no interaction) the solution of (11) is

$$a(z) = a(o)e^{ik_{zo}z} \tag{15}$$

giving back (considering also (12) and (13)) the uncoupled mode (10).

In order to complete the analysis of any particular free electron laser scheme, the alternating current $\underline{J}(x,y,z)$ which is induced by the electromagnetic wave in the electron beam should be calculated by solving the electron equations (force equation, Vlasov equation, Dirac equation or other) in the particular structure considered. In the linear regime this will usually lead to a linear relation between the current and the electromagnetic field. Equiped with such a relation it would be usually straightforward to solve the linear equations (11,12) by a Laplace transform technique.

This procedure was used successfully on both Cerenkov-Smith-Purcell [20,21] and longitudinal electrostatic bremsstrahlung [11] FELs. The Laplace transformed

amplitude of the electromagnetic wave $\bar{a}(s) = \int_0^\infty e^{-sz}\, a(z)dz$ was found in either case to be given by the same expression

$$\bar{a}(s) = \frac{1 + \chi(\omega, s + ik_o)/\varepsilon}{(s-ik_{zo})[1 + \chi(\omega, s+ik_o)/\varepsilon] - i\alpha\, \chi(\omega, s+ik_o)/\varepsilon}\, a(o) \tag{16}$$

where

$$\chi(\omega, s+ik_o) = (1+\alpha^2)\, \chi_p(\omega, s+ik_o) \tag{17}$$

$\chi_p(\omega,s)$ is the well known plasma susceptibility of an electron beam plasma propagating in free space in the z direction. It is defined by

$$\chi_p(\omega,s) = -i\, \frac{e^2}{\varepsilon} \iiint_{-\infty}^{\infty} \frac{g^{(o)}(p_x,p_y,p_z)/\partial p_z}{s - i\,\omega/v_z}\, dp_x dp_y dp_z \tag{18}$$

$g^{(o)}$ is the electron distribution function of the electron beam when entering the interaction region, $v_z = p_z/(\gamma m)$ is the electron longitudinal velocity component.

The parameter α^2 in Eq. (17) is equal zero for all FELs discussed except the longitudinal electrostatic bremsstrahlung FEL for which it was found to be[11]:

$$\alpha^2 = \left(\frac{1}{2\beta_o^2\gamma_o^3}\right) \left(\frac{\omega_p}{\omega}\right)^2 \left(\frac{e\varepsilon_o}{mc^2}\right)^2 \tag{19}$$

where $\Phi_o = E_o/k_o$ is the amplitude of the periodic electrostatic potential in this laser.

In Eq. (16) k_o is the periodicity parameter which is given for all FELs except the Cerenkov FEL by Eq.1. In the Cerenkov FEL, which does not utilize a periodic structure, one uses $k_o = 0$.

The coupling parameter κ is listed in Table 2 for the various kinds of FELs. A_e is the thin electron beam cross section area. x_e, y_e are the transverse coordinates of this beam. $\mathcal{E}_{z1}(x,y)$, which appears in row 2 of the table, is the longitudinal electric field profile of the first order space harmonic of the electromagnetic mode in the Smith-Purcell FEL periodic waveguide

$$\mathcal{E}_{z1}(x,y) = \frac{1}{L}\int_0^L e^{-ik_o z}\,\mathcal{E}_z(x,y,z)\,dz \qquad (20)$$

Table 2 : The coupling parameter κ of various FELs (the highly relativistic limit expressions are given in brackets).

FEL	κ
Cerenkov	$\dfrac{\frac{1}{2} A_e \sqrt{\varepsilon/\mu}\ \lvert \mathcal{E}_{zo}(x_e,y_e) \rvert^2}{P} \dfrac{\Pi}{\lambda}$
Smith-Purcell	$\dfrac{\frac{1}{2} A_e \sqrt{\varepsilon/\mu}\ \lvert \mathcal{E}_{z1}(x_e,y_e) \rvert^2}{P} \dfrac{\Pi}{\lambda}$
Long. Elec.	$\alpha^2 \dfrac{\frac{1}{2} A_e \sqrt{\varepsilon/\mu}\ \lvert \mathcal{E}_{zo}(x_e,y_e) \rvert^2}{P} \dfrac{\Pi}{\lambda}$
Trans. Elec.	$\dfrac{1}{8\pi} \left(\dfrac{eE_o}{mc^2}\right)^2 \dfrac{(1+\beta_{oz})^2}{\beta_{oz}^2} \dfrac{\gamma_{oz}^4}{\gamma_o^2} \dfrac{A_e}{A_g} \lambda \quad \left[\dfrac{1}{2\pi}\left(\dfrac{eE_o}{mc^2}\right)^2 \dfrac{\gamma_{oz}^4}{\gamma_o^2} \dfrac{A_e}{A_g} \lambda\right]$
Mag.Brem.	$\dfrac{1}{8\pi} \left(\dfrac{eB_o c}{mc^2}\right)^2 (1+\beta_{oz})^2 \dfrac{\gamma_{oz}^4}{\gamma_o^2} \dfrac{A_e}{A_g} \lambda \quad \left[\dfrac{1}{2\pi} \left(\dfrac{eB_o c}{mc^2}\right)^2 \dfrac{\gamma_{oz}^4}{\gamma_o^2} \dfrac{A_e}{A_g} \lambda\right]$
Compton-Raman	$\left[\dfrac{2}{\pi} \left(\dfrac{eE_o}{mc^2}\right)^2 \dfrac{\gamma_{oz}^4}{\gamma_o^2} \dfrac{A_e}{A_g} \lambda = \dfrac{4}{\pi} \left(\dfrac{e}{mc^2}\right)^2 \left(\dfrac{\varepsilon_o}{\varepsilon_o}\right)^{1/2} S_o \dfrac{\gamma_{oz}^4}{\gamma_o^2} \dfrac{A_e}{A_g}\right]$

It is instructive to find out that Cerenkov, Smith-Purcell and longitudinal electrostatic bremsstrahlung FELs all have similar expressions for the coupling coefficient κ. This stems from the fact that they all involve direct longitudinal interaction of an electromagnetic wave component with a synchronous electron plasma wave component. In the Cerenkov scheme the z component of the total electromagnetic mode field $\underline{\mathcal{E}}(x,y)$ can be synchronized and coupled to electron plasma waves. In the Smith-Purcell (or traveling wave tube) type scheme only the electromagnetic mode first order, space harmonic $\underline{\mathcal{E}}_1(x,y)$ is synchronous with the electron plasma waves. In the longitudinal electrostatic bremsstrahlung scheme the total electromagnetic mode $\underline{\mathcal{E}}(x,y)$ is synchronous with only the -1 order space harmonic of the electron plasma wave which has an amplitude α (Eq. 19). In all three cases the coupling coefficient is proportional to the radiation wavenumber $k = 2\pi/\lambda$ and to "relative power" factors of the interacting wave components.

The dispersion-gain relation (16) applies to a good approximation also to the case of magnetic bremsstrahlung FEL. Assuming operation near synchronism, and introducing a "relative power" factor (*filling factor*) A_e/A_g (A_g is the waveguide cross section area or more generally the effective cross section of the electromagnetic mode), we were able to reduce the dispersion equation developed in [10] for the magnetic bremsstrahlung laser to a form identical with (16). The coupling coefficient κ which results for this case is listed in Table 2 row 5. B_0 in this expression is the amplitude of the periodic magnetic field modulation. Notice that for the magnetic bremsstrahlung FEL as well as

for the other transverse modulation FELs the electron distribution function $f_o(p_x,p_y,p_z)$ has an average transverse momentum $p_{o\perp} \neq 0$ (while for the longitudinal FELs $p_{o\perp} = 0$). In the magnetic bremsstrahlung case

$$p_{o\perp} = \sqrt{p_{ox}^2 + p_{oy}^2} = \frac{eB_o}{k_o} \tag{21}$$

thus, in the velocity space, the average longitudinal velocity of the beam will be given by

$$v_{oz} = \frac{p_{oz}}{\gamma_o m} = \frac{1}{\gamma_o m}\sqrt{p_o^2 - p_{o\perp}^2} \tag{22}$$

The transverse electrostatic bremsstrahlung FEL scheme is essentially equivalent to the magnetic bremsstrahlung FEL except that a periodic transverse electrostatic force is applied on the electrons by periodic alternating electrodes replacing the periodic magnetic (Lorentz) force which is applied in the magnetic bremsstrahlung FEL by means of static magnets or coils. It was also suggested that high amplitude electrostatic field modulation can be obtained due to the change in the space charge field of an electron beam traversing through a periodically rippled waveguide, and that this can be utilized for a free electron laser scheme.[12,28]

It is possible to avoid a detailed analysis of the transverse electrostatic bremsstrahlung laser scheme, using a reasonable assumption that the electrons respond to the periodic transverse electric force eE_o in the same way that they respond to the transverse magnetic (Lorentz) force $e\underline{B}_o \times \underline{v}_z$. We thus will assume that the existing theory of the magnetic bremsstrahlung FEL can be applied to a good approximation to the transverse electrostatic bremsstrahlung FEL when we

substitute $B_o v_z$ by E_o, where E_o is the amplitude of the transverse electrostatic field modulation. Hence Eq.16 will hold for the transverse electrostatic bremsstrahlung laser as well, with the coupling parameter κ given in Table 2 row 4 and χ_p defined by (18). Instead of (21) we should use in this case

$$p_{o\perp} = \frac{eE_o}{k_o v_{oz}} \tag{23}$$

In the Compton-Raman FEL the electron beam is pumped by both the transverse electric and magnetic fields of an electromagnetic wave propagating in counter direction to the electron beam. The dispersion relation which results from the analysis of this interaction [16] can be also reduced to the general form (16). The analysis of Ref.[16] is limited to small transverse oscillation ($\gamma_{oz} \simeq \gamma_o$). However at least in the highly relativistic limit the parameter κ can be directly derived from the expressions for the magnetic bremsstrahlung laser taking advantage of the fact that in this limit a static magnetic field and an electromagnetic wave look alike in the beam moving frame, and using the appropriate synchronism condition for this case (8 or 9). In Eq. 16 one should substitute then $\omega - k_o$ of ω.

The coupling coefficient κ for the Compton-Raman scattering FEL is given in Table 2 row 6 in the limit of a highly relativistic beam. This is actually the more interesting case because only in this limit the laser can produce radiation at a wavelength appreciably shorter than the pump ($\lambda \simeq \lambda_o/(4\gamma_{oz}^2)$). The parameter χ is also given in terms of the power density value of the pump field S_o.

The common gain-dispersion relation (16) would yield the power gain for any FEL at any wavelength when $\tilde{a}(s)$ is inverse Laplace transformed and substituted in

$$\frac{P(z)}{P(o)} = \left| \frac{a(z)}{a(o)} \right|^2 \tag{24}$$

The operating wavelength is determined from the solution of the dispersion equation which is the condition for the vanishing of the denominator in (16).

$$(s-ik_{zo})[1 + \chi(\omega, s+ik_o)/\varepsilon] - i\kappa\chi(\omega, s+ik_o)/\varepsilon = o \tag{25}$$

For a weakly coupled system (κ is small), the eigenmodes of the system have wavenumbers close to the eigenmodes of the uncoupled system ($\kappa=o$) which are the electromagnetic wave ($s = ik_{zo}$) and the electron beam plasma waves (solutions of the plasma dispersion equation : $1 + \chi/\varepsilon = o$). The approximate wavenumbers of these waves (more precisely - the wavenumbers of the space harmonics which participate in the interaction), are listed in Table 1, giving rise to the radiation conditions listed in the third column of the table. When the wavenumbers of the interacting waves match (synchronism), the dispersion equation (25) vanishes and the appearance of a pole in (16) indicates strong coupling of the electron plasma and electromagnetic waves. We should point out that Eq.16 and the parameters in Table 2 were all derived with the assumption

of operation near synchronism.

The susceptibility function $\chi(\omega,s)$ (Eqs.17,18) can be expressed in terms of familiar functions and parameters. The distribution function $g^{(o)}(\underline{p})$ may be substituted in terms of a normalized distribution function of a single variable:

$$g^{(o)}(p_z) = \frac{p_{zth}}{n_o} \int\int_{-\infty}^{\infty} g^{(o)}(p_x,p_y,p_z)\, dp_x dp_y \equiv \frac{n_o}{p_{zth}}\, \bar{g}\left(\frac{p_z-p_{oz}}{p_{zth}}\right) \tag{26}$$

where n_o is the electron beam density, p_{zth} -the longitudinal momentum spread of the electron beam distribution, and p_{oz} is the average electron beam momentum in the longitudinal (z) direction. In terms of the normalized function $\bar{g}$, the plasma susceptibility (18) can be written as

$$\chi(\zeta,s)/\zeta = \frac{1}{2}\cdot\frac{k_D'^2}{s^2}\, G'(\zeta) \tag{27}$$

where

$$G(\zeta) \equiv \int_{-\infty}^{\infty} \frac{\bar{g}(x)}{x-\zeta}\, dx \tag{28}$$

$$\equiv \frac{i\omega/s - v_{oz}}{v_{zth}'} \tag{29}$$

$$k_D'^2 \equiv 2\,\frac{\omega_p'^2}{v_{zth}'^2} \tag{30}$$

$$\omega_p'^2 = (1+\alpha^2)\frac{\omega_p^2}{\gamma_o\gamma_{oz}^2} = \frac{1+\alpha^2}{\gamma_o\gamma_{oz}^2}\frac{e^2 n_o}{m\varepsilon} \tag{31}$$

$$v_{zth}' = \frac{p_{zth}}{\gamma_o\gamma_{oz}^2 m} = \frac{E_{zth}}{\gamma_o\gamma_{oz}^2\beta_{oz}mc} \tag{32}$$

E_{zth} is the longitudinal kinetic energy spread of the electron beam. In stimulated Compton Raman scattering substitute [illegible].

Often the electron distribution is approximated by a shifted Maxwellian distribution.

For this case

$$\bar{g}(x) = \frac{1}{\sqrt{\pi}}\, e^{-x^2} \tag{33}$$

and

$$G(\zeta) = \frac{1}{\sqrt{\pi}} \int_{-\infty}^{\infty} \frac{e^{-x^2}}{x-\zeta}\, dx \tag{34}$$

is the so called plasma dispersion function which is tabulated in Ref.[29].

Before we go to the next section where the solution of (16,25) and the laser gain regimes are discussed, let us examine Eq.25, in the limit of a cold beam ($p_{zth} \to 0$). In this limit we get from (29,28) [illegible] and $G'(\zeta) \to 1/\zeta^2$. Substitution in (27) and (16) gives

$$\chi(\omega,s) = \varepsilon \frac{\omega_p'^2}{(\omega+iv_{oz}s)^2} \tag{35}$$

$$\bar{a}(s) = \frac{(s + ik_o - i\frac{\omega}{v_{oz}})^2 + \frac{\omega_p'^2}{v_{oz}^2}}{(s - ik_{zo})\left[(s+ik_o - i\frac{\omega}{v_{oz}})^2 + \frac{\omega_p'^2}{v_{oz}^2}\right] - i\kappa\frac{\omega_p'^2}{v_{oz}^2}} a(o) \tag{36}$$

and the dispersion relation (25) is

$$(s - ik_{zo})\left[(s + ik_o - i\frac{\omega}{v_{oz}})^2 + \frac{\omega_p'^2}{v_{oz}^2}\right] - i\kappa\frac{\omega_p'^2}{v_{oz}^2} = 0 \tag{37}$$

This equation is similar to the conventional traveling wave tube dispersion equation [30]. Its physical significance is seen when we take the limit $\kappa = o$ (no interaction). We see that the uncoupled eigenmodes of the system in the cold beam limit are the electromagnetic wave

$$s = i\,k_{zo} \tag{38}$$

and the slow and fast plasma waves (correspondingly)

$$s + i\,k_o = i\left(\frac{\omega}{v_{oz}} + \frac{\omega'_p}{v_{oz}}\right) \tag{39}$$

$$s + i\,k_o = i\left(\frac{\omega}{v_{oz}} - \frac{\omega'_p}{v_{oz}}\right) \tag{40}$$

The dispersion relation (37) can be further simplified into the compact form

$$\delta k \quad (\delta k - \quad - \theta_p)(\delta k - \theta + \theta_p) + Q = 0 \tag{41}$$

where we defined the complex wave number modification due to coupling - δk, by

$$\quad i k_{zo} + i \quad k \tag{42}$$

the [illegible] parameter:

(43)

[illegible] Raman scattering)

the [illegible] parameter:

$$\quad p \quad v_{oz} \tag{44}$$

and the gain parameter

$$Q \quad \frac{\quad^2}{v_{oz}^2} = \quad \quad p^2 \tag{45}$$

4. FREE ELECTRON LASER GAIN REGIMES

In principle the calculation of the gain of any FEL at arbitrary operating conditions is straightforward, requiring only to perform an inverse Laplace transform of (16), then using (24) and the appropriate coupling parameter from Table 2. In practice the execution of an inverse Laplace transorm may be somewhat difficult in the general case ($p_{zth} \neq o$) where the exact plasma dispersion function (28 or 34) must be used in (27). In this general case it may be most useful to evaluate the inverse transform

$$a(z) = \frac{1}{2\pi i} \int_{\gamma - i\infty}^{\gamma + i\infty} \bar{a}(s) e^{sz} ds \qquad (46)$$

by numerical integration in the complex field. A computer program for performing this integral was developed [21]. Representative gain curves calculated by this program are shown in Fig. 3. As a function of the interaction-length-normalized-synchronizm-parameter $\bar{\delta}$:

$$\bar{\delta} = \ell = \left(\frac{\omega}{v_{oz}} - k_{zo} - k_o\right) \ell \qquad (47)$$

and various values of the normalized thermal spread parameter $\bar{\theta}_{th}$

$$\bar{\theta}_{th} = \frac{\omega}{v_{oz}} \frac{v'_{zth}}{v_{oz}} = \frac{2\pi}{\bar{\delta}_{oz}} \frac{v'_{zth}}{v_{oz}} \frac{1}{\ell} \qquad (48)$$

$$\bar{\theta}_{th} = \theta_{th}\ell = \frac{2\pi}{\beta_{oz}} \frac{v'_{zth}}{v_{oz}} \frac{\ell}{\lambda} \tag{49}$$

The thermal spread parameter $\bar{\theta}_{th}$ has the interpretation as the spectral width (evaluated in wave number space) of electron wave numbers $\Delta\left(\frac{\omega}{v_z}\right)$ in an electron beam with average longitudinal velocity v_{oz} and velocity spread v'_{zth}. As we will see later in this section the beam is considered cold or warm if $\bar{\theta}_{th} \ll 1$ or $\bar{\theta}_{th} \gg 1$ respectively. Fig. 3 displays examples in both limits as well as intermediate cases. The normalized coupling and space charge parameter $\bar{\kappa}$ and $\bar{\theta}_p$ which appear in Fig. 3 are defined by

$$\bar{\kappa} = \kappa\ell \tag{50}$$

$$\bar{\theta}_p = \theta_p \ell = \frac{\omega_p'}{v_{oz}} \ell \tag{51}$$

In many practical limits exact calculation of the gain curve is not necessary and analytical expressions for the gain may be derived with certain approximations. These different limits (gain regimes) were delineated by a number of authors [4,7,10,17,18,20] for various kinds of FELs. Indeed they are common to all of them, since they result from the same gain-dispersion relation (16). We will briefly describe the gain characteristics in these regimes.

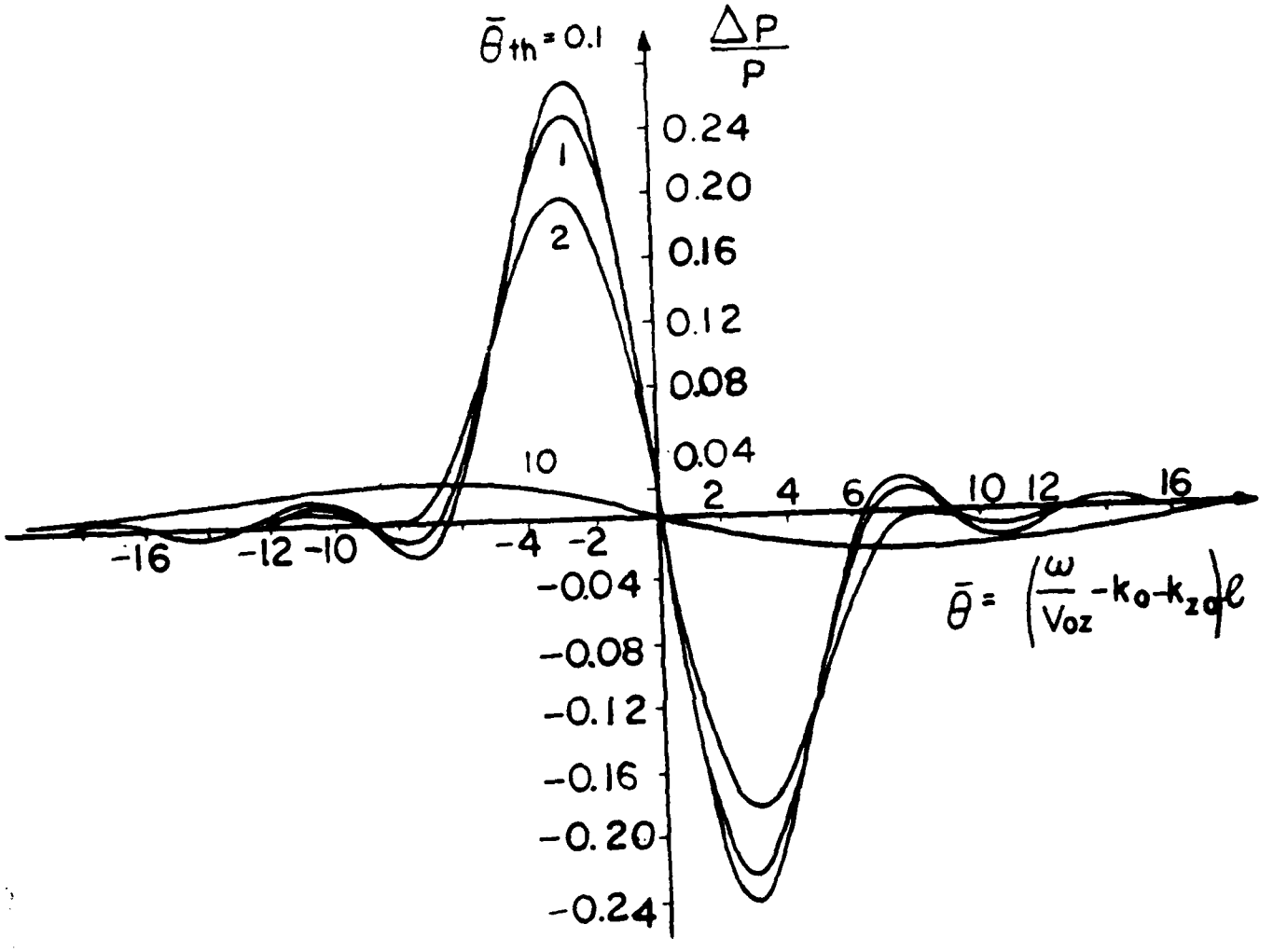

Fig. 3: Numerically calculated gain curves of the FEL for various values of the normalized thermal spread parameter $\bar{\gamma}_{th}$ ($\bar{\kappa} = 1$, $\bar{\gamma}_z = 1$).

Fig. 4 displays "phase matching" (momentum conservation) diagrams which help to understand the various gain regimes discussed. It is essentially a "blow up" of the phase matching diagram in Fig. 2 (b), looking at the details of the phase matching near the electron waves dispersion curve at the various gain regimes. In the bremsstrahlung FELs, k_o in Fig. 4 is reversed in direction. Also in the stimulated Compton-Raman scattering $k_o = \omega_o/c$ is reversed and $\omega/v_{oz} \to (\omega - \omega_o)/v_{oz}$. In the cerenkov FEL $k_o = o$. The other details remain the same in all FELs.

Cold beam low gain regime

As was shown in the previous section, in the cold beam limit $(p_{zth} \to o)$ the dispersion equation (35) reduces to (37) or (41) which are simple third degree polinomial equations with a finite number of roots (three). If the roots are found, then the evaluation of the inverse Laplace transform (46) may be straightforwardly calculated by use of the residuum method. This gives

$$\frac{a(z)}{a(o)} = \sum_{j=1}^{3} A_j e^{s_j z} \tag{52}$$

where A_j are the residues of (36) at s_j.

The low gain regime occures at the limit when the normalized gain parameter $\bar{Q}$ is very small: $\bar{Q} \ll 1$ (a sufficient condition).

$$\bar{Q} = \bar{\vartheta}_p^2 = Q\beta^3 \tag{53}$$

In this limit the roots of (37) and (41) will be close to the roots of the

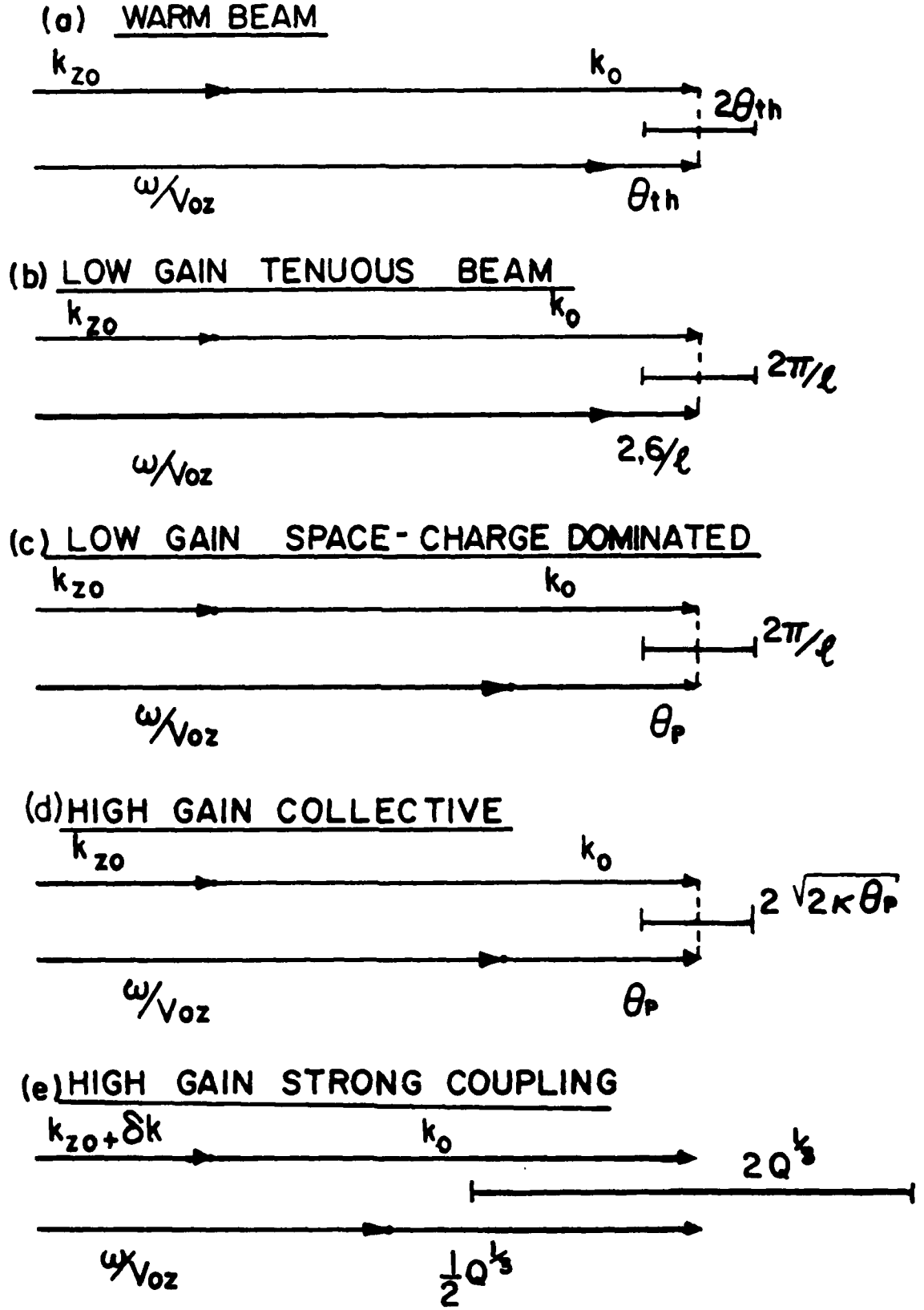

Fig. 4: "Phase matching" (momentum conservation) diagrams at the different gain regimes assuming operation at the maximum gain point. The section under each diagram indicates the width of the gain region.

uncoupled waves ($Q = o$) - Eqs. 38 - 40, and may be expanded to first order in κ or Q around this zero order values. After a lengthy mathematical calculation, [21] substituting (52) in (24), and calculating the power output to first order in κ (or Q), one gets

$$\frac{\Delta P}{P(0)} = \bar{Q}\, F(\bar{\theta}, \bar{\theta}_p) \tag{54}$$

where $\Delta P = P(\ell) - P(0) \ll P(0)$, and

$$F(\bar{\theta}, \bar{\theta}_p) = \frac{1}{2\bar{\theta}_p}\left[\frac{\sin^2\left(\frac{\bar{\theta}+\bar{\theta}_p}{2}\right)}{\left(\frac{\bar{\theta}+\bar{\theta}_p}{2}\right)^2} - \frac{\sin^2\left(\frac{\bar{\theta}-\bar{\theta}_p}{2}\right)}{\left(\frac{\bar{\theta}-\bar{\theta}_p}{2}\right)^2}\right] \tag{55}$$

The function $F(\bar{\theta}, \bar{\theta}_p)$ is shown in Fig. 5 for various values of the parameter $\bar{\theta}_p$ (51). Since $F(\bar{\theta}, \bar{\theta}_p) < 1$ the parameter $\bar{Q}$ indicates an upper limit on the power gain available.

Eqs. 54, 55 give the low gain characteristics of free electron lasers <u>including space charge effect.</u> For a tenuous beam or a short interaction length $\bar{\theta}_p \ll \pi$ and (55) reduces to

$$F(\bar{\theta}, 0) = \frac{d}{d\bar{\theta}}\left[\frac{\sin(\bar{\theta}/2)}{\bar{\theta}/2}\right]^2 \tag{56}$$

which is the familiar single electron gain function which appears in the analyses of the various free electron lasers where space charge effect is neglected [3-5, 10, 13, 20]. Notice also that the gain curve for this case (Fig. 5, $\bar{\theta}_p = o$) resembles the computer calculated curve of Fig. 3 for

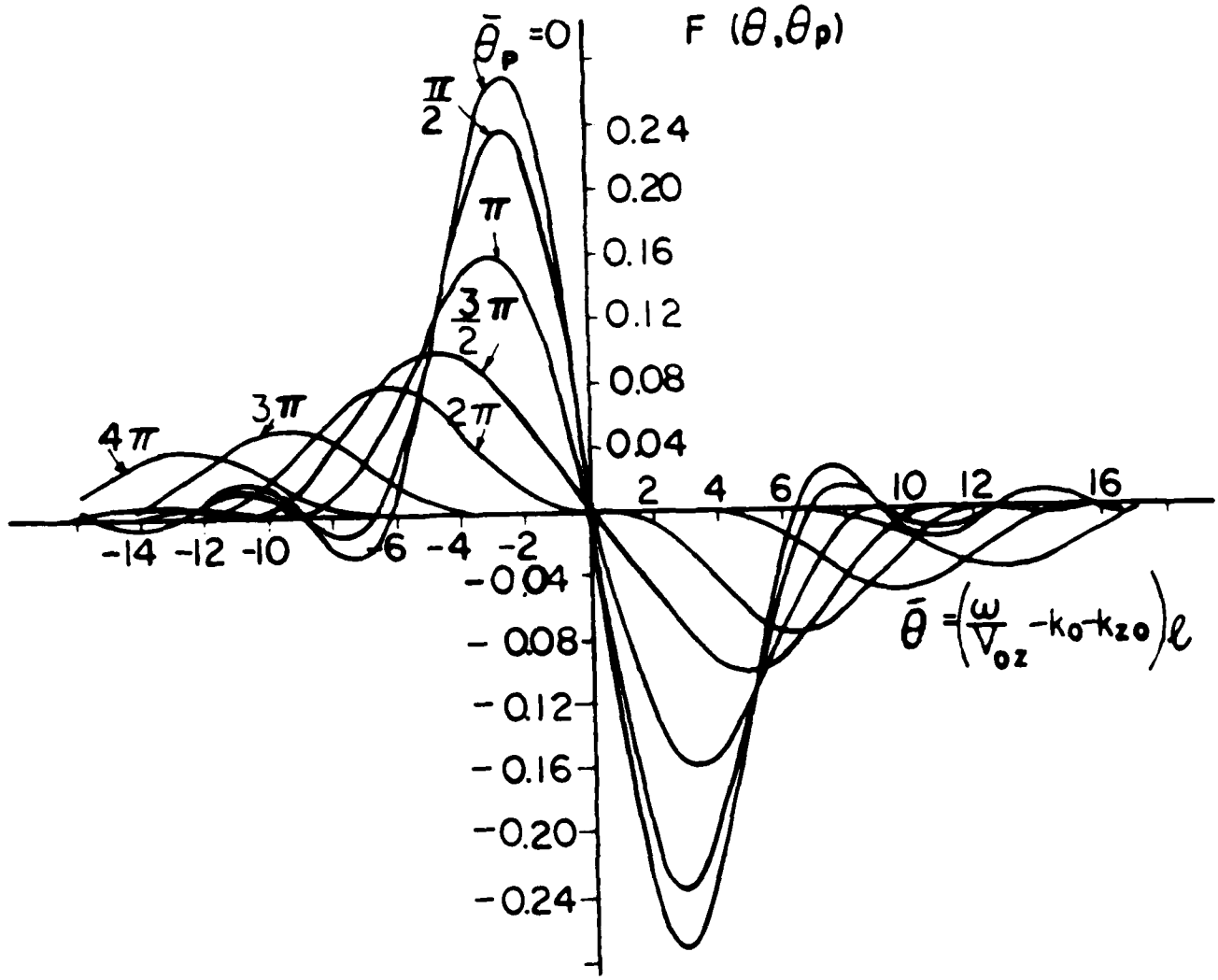

Fig. 5: The normalized low gain curves $F(\bar{\theta}, \bar{\theta}_p)$ (Eq. 55) for various values of the normalized space charge parameter $\bar{\theta}_p$.

$\bar{\delta}_{th} = 0.1 \ll 1$ (cold beam). It attains its maximum value at

$$\bar{\omega} = -\frac{2.6}{\bar{\beta}} \quad \text{or} \quad \frac{\omega}{v_{oz}} + \frac{2.6}{\beta} = k_{zo} + k_o \tag{57}$$

This situation is illustrated in Fig. 4(b).

It is interesting to point out that the expression which was derived by Lousiell et all [31] for the magnetic bremsstrahlung FEL gain in the low gain regime including space charge effect, is actually just the Taylor expansion of (55) to first order in $\bar{\theta}_p^2$:

$$F(\bar{\omega}, \bar{\theta}_p) = \frac{d}{d\bar{\omega}} \left[\frac{\sin(\bar{\omega}/2)}{\bar{\omega}/2}\right]^2 + \frac{\bar{\theta}_p^2}{6} \frac{d^3}{d\bar{\omega}^3} \left[\frac{\sin(\bar{\omega}/2)}{\bar{\omega}/2}\right]^2 \tag{58}$$

This expansion is correct of course only for $\bar{\theta}_p \ll \pi$.

The general space charge limited expression (55) has the interesting physical interpretation as the result of the interference of the electromagnetic wave (38) with the slow space charge wave (39) on one hand and with the fast space charge wave (40) on the other hand. Whenever the electromagnetic wave is synchronous with the slow space charge wave ($\omega = \omega_p$ or $k_{zo} + k_o = \frac{\omega}{v_{oz}} + \theta_p$), the interference yields maximum net gain. When the electromagnetic wave is synchronous with the fast space charge wave ($\omega = -\omega_p$ or $k_{zo} + k_o = \frac{\omega}{v_{oz}} - \theta_p$) maximum attenuation is obtained. The phase matching diagram in the space charge dominated low gain regime ($\bar{\theta}_p \gg \bar{\delta}$) at the maximum gain point :

$$\omega = -\bar{\theta}_p \quad \text{or} \quad \frac{\omega}{v_{oz}} + \theta_p = k_{zo} + k_o \tag{59}$$

is shown in Fig. 4(c).

The gain expression (54) may be of practical importance in situations when low gain operation is expected (as in laser oscilators), and weak coupling parameter (κ) is unavoidable (as in the case of short wavelength operation). In this situation one may try to increase the gain parameter $\bar{Q}$ (53) by increasing the electron density and the interaction length ℓ, thus arriving to the regime $\bar{\theta}_p >> \pi$. For example with beam parameters $n_o = 10^{11}$ cm^{-3}, $\gamma_o = \gamma_{oz} = 10$, $v_{oz} \simeq c$, and $\ell = 2$ m one gets $\bar{\theta}_p \simeq 5$, and it is necessary to use (55) to describe the gain.

When we are in the space-charge dominated limit $\bar{\theta}_p >> \pi$ at the maximum gain point (59), the normalized gain function (55) attains a value $F(-\bar{\theta}_p, \bar{\theta}_p) = 1/(2\bar{\theta}_p)$. Thus the maximum gain (54, 55) is given by.

$$\left(\frac{\Delta P}{P}\right)_{max} = \frac{\bar{Q}}{\bar{\theta}_p/2} = 2\kappa\theta_p \ell^2 \tag{60}$$

we notice that in this low gain space charge dominated regime the gain grows proportionally to $\sqrt{n_o}$ while in the tenuous beam limit (56) where collective effects were negligible, the gain was proportional to n_o (single electron interaction). Notice also that since $\bar{\theta}_p >> \pi$ was assumed, the parameter $\bar{Q}$ gives again an upper limit on the gain available.

It should be pointed out here that as the electron density is increased, and space charge effects become important, saturation (trapping) effect would start at a lower input power level of the electromagnetic radiation. In this case the linear analysis which led to (54) may fail to describe the situation with practical power levels, and a complete nonlinear analysis should be used [32,33]

Cold beam high gain collective (Raman) regime

For weak enough coupling ($\tilde{Q} \ll 1$) the roots of (41) are all real and small, thus the roots s_j (Eq. 42) are all imaginary and close to the uncoupled wave numbers (38 - 40), and give rise to the "interferential" gain expression (54,55). As $\tilde{Q}$ is increased, the polynomial equation (41) starts having one real and two complex (conjugate) solutions. Consequently, one of the roots s_j (Eq. 42) must have positive real part (corresponding to gain) and the other two have a negative and a vanishing real part (corresponding to loss and a constant amplitude respectively). In this limit - "the high gain limit" - we can neglect the interference between the different roots, in (52), (24), and keep only the exponentially growing wave. Then from (24)

$$\ln \frac{P(\ell)}{P(0)} \simeq 2\ell n|A_j| + 2(\mathrm{Res}_j)\,\ell \simeq 2(\mathrm{Res}_j)\ell = -2\,(\mathrm{Im}\delta k)\ell \qquad (61)$$

where s_j is the exponentially growing root.

In the particular case when the electromagnetic wave is synchronous with the slow space charge wave:

$$\delta = -\theta_p \qquad \text{or} \qquad \frac{\omega}{v_{oz}} + \theta_p = k_{zo} + k_o \tag{62}$$

and assuming $|\delta k| << \theta_p$, Eq. 41 may be approximated by a simple second degree equation

$$(\delta k)^2 = -\frac{Q}{2\theta_p} \tag{63}$$

The root of this equation which corresponds to a growing wave is $\delta k = -i\sqrt{Q/2\theta_p}$, and substituting in (61) it gives

$$\ln \frac{P(\ell)}{P(0)} = \left(\frac{2\bar{Q}}{\bar{\theta}_p}\right)^{1/2} = (2\kappa\ell_p)^{1/2} \tag{64}$$

This gain regime is often termed as the stimulated Raman regime since it involves stimulated scattering of the electromagnetic wave by the slow space charge plasma wave [4,10,34,35,36]. The phase matching diagram of these waves (Eq. 62) is shown in Fig. 4(d).

In this gain regime the gain grows with electron density proportionally to $n_o^{1/4}$. Also we point out that the derivation of (64) required the constraints $\bar{\theta}_p >> |\mathrm{Im}\delta k\ell| >> 1$, thus we see from (64) that the parameter $\sqrt{\bar{Q}}$ gives an upper limit of the gain available in this regime.

Cold beam - high gain - strong coupling regime

In the limit of high gain and strong coupling ("strong pump") the FEL parameters satisfy $Q^{1/3} >> \theta_p$ (or equivalently : $\kappa >> \theta_p$). Near

synchronizm

$$\delta = 0 \quad \text{or} \quad \frac{\omega}{v_{oz}} = k_{zo} + k_o \tag{65}$$

δ and ω_p are negligible relative to δk_i in Eq. 41, which reduces then into a straightforwardly soluble third degree polinomial equation

$$(\delta k)^3 = - Q \tag{66}$$

The root of this equation which corresponds to a growing wave is

$$\delta k = \frac{1 - i\sqrt{3}}{2} Q^{1/3} \tag{67}$$

and using (61) it gives

$$\ln \frac{P(\ell)}{P(o)} = \sqrt{3}\, \bar{Q}^{1/3} = \sqrt{3}\, (k\omega_p^2)^{1/3} \ell \tag{68}$$

Hence in this gain regime the parameter $\bar{Q}$ solely determines the available power gain. The gain depends on the electron beam density in proportion to $n_o^{1/3}$.

Eq. 67 indicates that the real part of the wave number k_{zo} changes appreciably due to the interaction (by $\mathrm{Re}\delta k$). Instead of (65) it would be preceptive to draw the phase matching diagram at the maximum gain point

(Fig. 4e) in terms of the modified wave number k_{zo} + Reδk

$$\text{Re}\delta k = \frac{1}{2} Q^{1/3} \quad \text{or} \quad \frac{\omega}{v_{oz}} + \frac{1}{2} Q^{1/3} = (k_{zo} + \text{Re}\delta k) + k_o \tag{69}$$

Warm beam high gain regime

In deriving the cold beam dispersion and gain relations (36,37) we used an asymptotic expansion of (28) which is valid only for $|\zeta| >> 1$. If this condition is not satisfied, one has to go back and solve (25) with the plasma susceptibility given by (27,28) and not by (35).

Using (42) in (29), the parameter ζ may be written around $s = ik_{z0}$ in terms of the detuning parameter θ (43):

$$\zeta = \frac{\theta - \delta k}{\theta_{th}} \tag{70}$$

where θ_{th} is defined by (48). If $\bar{\theta}_{th} = \theta_{th}(\zeta) >> \text{Im}\delta k$ (which later yields $\theta_{th}^3 >> Q$) and $\theta_{th} >> \theta_p$ (which is equivalent to $k_{zo} + k_o >> k_D'$ - the space charge wave number is much shorter than the Debye length), then it follows from (70) that the requirement $|\zeta| = |(\theta - \text{Re}\delta k)^2 + (\text{Im}\delta k)^2| / \theta_{th}^2 >> 1$ cannot be satisfied at any of the synchronizm conditions required for the gain regimes previously discussed. In these conditions we are bound to look for gain in the regime $|\zeta| \leq 1$ and solve (25) with $\chi(\omega, s)$ given by (27,28).

With small enough coupling coefficient κ, it is possible again to solve the dispersion equation (25) by means of a first order expansion of the roots in terms of κ. In the conditions stated above it is possible to show that apart for the electromagnetic-like root (38), all the other zero order solutions of the dispersion equation are complex, corresponding to plasma waves which decay strongly by Landau damping. It is sufficient then to consider only the isolated root $s = ik_{zo}$ (38) which would given an exponentially growing wave.

The first order expansion of (25) around $s = ik_{zo}$ gives

$$\text{Res} = -\delta k_i \simeq \frac{\kappa}{2} \frac{k'^2_D}{(k_{zo}+k_o)^2} \frac{\text{Im } G'(\zeta)}{\left|1 - \frac{1}{2} \frac{k'^2_D}{(k_{zo}+k_o)^2} G'(\zeta)\right|^2} \tag{71}$$

where $\delta k_i \equiv \text{Im}\delta k$, and ζ is given by (70).

$$\zeta = \zeta_r + i\zeta_i \tag{72}$$

$$\zeta_r = \frac{v - \text{Re}\delta k}{\theta_{th}} \simeq \frac{v}{\theta_{th}} \tag{73}$$

$$\zeta_i \simeq -\frac{\delta k_i}{\theta_{th}} \tag{74}$$

From the definition (28) we have

$$\mathrm{Im}\, G'(\zeta) = \int_{-\infty}^{\infty} g'(x)\, \frac{\zeta_i}{(x-\zeta_r)^2+\zeta_i^2}\, dx \tag{75}$$

Because of our initial assumptions $\zeta_i = |\delta k_i|/\bar{\theta}_{th} \ll 1$, the Lorentzian inside the integral (75) is much narrower than the function $g'(x)$. Hence $\mathrm{Im}\, g'(\zeta_r) \simeq \pi\, g'(\zeta_r)$

$$\mathrm{Im}\, G'(\zeta_r) \simeq \pi\, g'(\zeta_r) \tag{76}$$

Using the previously assumed inequality $k_D'^2 \ll k_{zo}+k_o$, (71) can be written in the form

$$\delta k_i \simeq -\frac{\kappa}{2}\, \frac{k_D'^2}{(k_{zo}+k_o)^2}\, \mathrm{Im}\, G'(\zeta_r) = -\frac{\bar{Q}}{\bar{\theta}_{th}^2}\, \mathrm{Im}\, G'(\zeta_r) \tag{77}$$

In terms of the detuning parameter θ the gain is given by [4,10,17,18,20]

$$\ln \frac{P(\ell)}{P(0)} = -2\delta k_i \ell = 2\, \frac{\bar{Q}}{\bar{\theta}_{th}^2}\, \mathrm{Im}G'\left(\frac{\theta}{\bar{\theta}_{th}}\right) = \frac{\bar{Q}}{\bar{\theta}_{th}^2}\, 2\pi g'\left(\frac{\theta}{\bar{\theta}_{th}}\right) \tag{78}$$

For a Maxwellian electron distribution (33) the imaginary part of the plasma dispersion function (76) is

$$\mathrm{Im}G'(\zeta_r) = -2\sqrt{\pi}\,\zeta_r e^{-\zeta_r^2} \tag{79}$$

This function is shown in Fig. 5. We see that it attains its maximum value when

$$\zeta_r = -1/\sqrt{2} \quad \text{or} \quad \omega = -\theta_{th}/\sqrt{2} \quad \text{or}$$

$$\frac{\omega}{v_{oz}} + \frac{1}{\sqrt{2}}\theta_{th} = k_{zo} + k_o \tag{80}$$

The diagram of this phase matching condition is shown in Fig. 4a.

At the maximum gain point (80) $\mathrm{Im}\,G'(-1/\sqrt{2}) = 1.5$, and the maximum gain is

$$\ln\frac{P(\ell)}{P(o)} = 3\,\frac{\bar{Q}}{\bar{\theta}_{th}^2} = 3\,\frac{\omega_p^2}{k_{th}^2} \tag{81}$$

Since we assumed initially $\bar{\theta}_{th} \gg 1$, again the parameter $\bar{Q}$ indicates an upper limit on the power gain available.

The warm beam regime is a regime of single electron interaction [17] and therefore the gain turned out to be proportional to the electron beam density n_o.

Warm beam low gain regime

Assuming in the low gain limit that $\kappa \to o$ and also that space charge effect can be neglected ($\theta_{th} \gg \theta_p$ or $k_{zo} + k_o \gg k_D'$), Eq. (16)

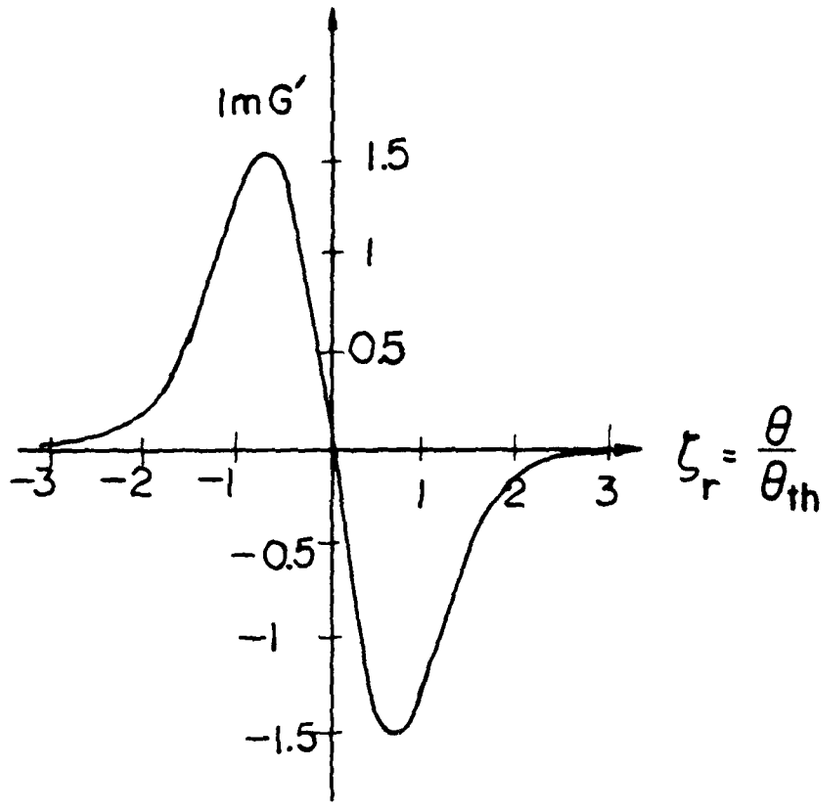

Fig. 6: The gain curve function Im $G'(\zeta_r)$ for a maxwellian distribution (Eq. 79).

reduces to

$$\bar{a}(s) = \left[\frac{1}{s-ik_{zo}} + \lim_{\cdot\to 0} \frac{i\cdot\chi(\cdot,s-ik_{zo})/\varepsilon}{(s-ik_{zo})(s-ik_{zo}+i\cdot)}\right] a(o) \tag{82}$$

By substituting (27) to (29) in (82) we get the explicit dependence of $\bar{a}$ (s) on s. The inverse Laplace transform (46) can be carried out now through the integral over x (or v_z) in the expression for χ (27,28), and evaluated by means of the residuum method. The result can be then substituted in (24), resulting after some tedious mathematical expansion (to first order in ε)

$$\frac{\Delta P}{P(0)} = \frac{\bar{Q}}{\bar{\beta}_{th}} \int_{-\infty}^{\infty} \frac{\sin^2(\bar{\theta}'/2)}{(\bar{\theta}'/2)^2} \bar{g}'\left(\frac{\bar{\theta}-\bar{\theta}'}{\bar{\beta}_{th}}\right) d\bar{\theta}' \tag{83}$$

This expression can be interpreted as a convolution between the warm beam gain curve $g'(\bar{\theta}/\bar{\beta}_{th})$ (78) and a spectral line shape function $\sin^2(\bar{\theta}/2)/(\bar{\theta}/2)^2$ which can be attributed to the wavenumber uncertainty due to the limite interaction length. When interaction by parts is applied to (84), the resulting expression will involve convolution between the cold beam gain curve $\frac{d}{d\bar{\theta}}\left[\sin^2(\bar{\theta}/2)/(\bar{\theta}/2)^2\right]$ (56) and a line shape function $\bar{g}\ (\bar{\theta}/\bar{\beta}_{th})$ which corresponds to line broadening due to electron velocity spread. Notice that the linear convolution relation (83) is applicable only in the limit of single electron interaction ($k_{zo} + k_o \gg k_D$) and low gain ($\Delta P/P(0) \ll 1$). However in the derivation of (83) there was no restriction on $\bar{\beta}_{th}$, and it would apply to both cold and warm beams as well as the intermediate regime.

In the limit $\bar{\nu}_{th} \ll 1$ (warm beam) the line shape function $\sin^2(\bar{\nu}/2)/[2^2(\bar{\nu}/2)^2]$ reduces to a delta function and (83) reduces to

$$\frac{\Delta P}{P(0)} = \frac{\bar{Q}}{\bar{\nu}_{th}^2} 2 - g' \left(\frac{\bar{z}}{\bar{\nu}_{th}}\right) \tag{84}$$

This expression is consistent with the high gain expression (78) which gives an identical result when we approximate $\ln[P(z)/P(0)] \simeq \Delta P/P(0)$. The high gain expression (78) thus applies in the low gain limit as well. The reason is that in the case we had, where the dispersion equation (25) had only a single significant root ($s \simeq ik_{2c}$), the high gain approximation (61) is correct at any gain level.

In the limit of a cold beam ($\bar{\nu}_{th} \ll 1$) Eq. (84) reproduces the low gain - cold beam limit expression (74, 76).

5. THE GAIN PARAMETER OF FELS

From the discussion above it appears that the normalized gain parameter $\bar{Q}$ (53) is a good figure of merit to characterize the gain of any free electron laser in all gain regimes (54, 60, 64, 68, 78, 83). While the maximum gain obtainable depends also on parameters which characterize the beam ($\bar{v}_p$, $\bar{\gamma}_{th}$) the dependence of the gain on the kind of FEL considered enters in all these equations only through the parameter $\bar{Q}$. Furthermore, the parameter $\bar{Q}$ indicates an upper limit of the gain in all regimes. As we increase $\bar{Q}$ by either increasing the coupling coefficient or the electron beam density, this upper limit grows at a declining rate from roughly $\bar{Q}$, through $\bar{Q}^{1/2}$ (if we go through the high gain collective regime) and finally as $\bar{Q}^{1/3}$. A simple necessary condition for obtaining appreciable gain in any FEL structure and any gain regime is $\bar{Q} > 1$.

In comparing the gain of various kinds of the free electron lasers discussed in this chapter, it is best to compare their normalized gain parameter $\bar{Q}$. This was calculated by substituting [illegible] from Table 2 in Eq. 53 and is presented in Table 3 for the various kinds of FELS.

TABLE 3: The normalized gain parameter $\bar{Q}$ for various FELs (the highly relativistic limit expressions are given in brackets).

Cerenkov $$4\pi^2 \frac{J_o}{e} \frac{r_e}{c} \frac{\ell^3}{\lambda} \frac{\frac{1}{2} A_e \sqrt{\epsilon_o/\mu_o} |\mathcal{E}_{zo}(x_e, y_e)|^2}{P} \frac{1}{\beta_o^3 \gamma_o^3}$$

Smith Purcell $$4\pi^2 \frac{J_o}{e} \frac{r_e}{c} \frac{\ell^3}{\lambda} \frac{\frac{1}{2} A_e \sqrt{\epsilon_o/\mu_o} |\mathcal{E}_{z1}(x_e, y_e)|^2}{P} \frac{1}{\beta_o^3 \gamma_o^3}$$

Long Elect. $$\pi \frac{J_o}{e} \frac{r_e^2}{c^2} \lambda \ell^3 \frac{\sqrt{\epsilon_o/\mu_o}\, E_o^2}{mc^2} \frac{A_e}{A_g} \frac{\sin^2\phi}{\cos\phi} \frac{1}{(1-\beta_o \cos\phi)^4} \frac{1}{\beta_o^5 \gamma_o^9}$$

$$\left[\frac{27}{16} \pi \frac{J_o}{e} \frac{r_e^2}{c^2} \lambda \ell^3 \frac{\sqrt{\epsilon_o/\mu_o}\, E_o^2}{mc^2} \frac{A_e}{A_g} \frac{\gamma_{oz}^2}{\gamma_o^3}\right]$$

Trans. Mag. $$2\pi \frac{J_o}{e} \frac{r_e^2}{c^2} \lambda \ell^3 \frac{\sqrt{\mu_o/\epsilon_o}\, H_o^2}{mc^2} \frac{A_e}{A_g} \frac{(1+\beta_{oz})^2}{\beta_{oz}^3} \frac{\gamma_{oz}^2}{\gamma_o^3}$$

$$\left[8\pi \frac{J_o}{e} \frac{r_e^2}{c^2} \lambda \ell^3 \frac{\sqrt{\mu_o/\epsilon_o}\, H_o^2}{mc^2} \frac{A_e}{A_g} \frac{\gamma_{oz}^2}{\gamma_o^3}\right]$$

Trans Elect. $$2\pi \frac{J_o}{e} \frac{r_e^2}{c^2} \lambda \ell^3 \frac{\sqrt{\epsilon_o/\mu_o}\, E_o^2}{mc^2} \frac{A_e}{A_g} \frac{(1+\beta_{oz})^2}{\beta_{oz}^5} \frac{\gamma_{oz}^2}{\gamma_o^3}$$

$$\left[8\pi \frac{J_o}{e} \frac{r_e^2}{c^2} \lambda \ell^3 \frac{\sqrt{\epsilon_o/\mu_o}\, E_o^2}{mc^2} \frac{A_e}{A_g} \frac{\gamma_{oz}^2}{\gamma_o^3}\right]$$

Compton Raman $$\left[64\pi \frac{J_o}{e} \frac{r_e^2}{c^2} \ell^3 \frac{S_o}{mc^2} \frac{A_e}{A_g} \frac{\gamma_{oz}^2}{\gamma_o^3}\right.$$

Since in many cases the current density J_o is a limiting factor, we expressed in Table 3 the modified plasma frequency in terms of the current density: $\omega_p^2 = eJ_o/(m_o v_{oz} \gamma_{oz}^3 \gamma_o)$. The parameter r_e which appears in the table is the classical electron radius:

$$r_e \equiv \frac{e^2}{4\pi\varepsilon_o mc^2} = 2.818 \times 10^{-15}\ \text{m} \tag{85}$$

The expression given for the longitudinal electrostatic bremsstrahlung FEL (row 3) is taken from Ref. [11]. The expression in brakets corresponds to the highly relativistic limit, assuming operation at an angle $\theta_m = (\sqrt{3}\gamma_o)^{-1}$ at which the gain parameter is maximal.

When one considers the dependence of the parameter $\bar{Q}$ on the operating parameters of the various FELs, it should be noticed that some of these parameters are dependent on each other. For example the wavelength λ, period L, velocity v_o and radiation angle θ depend on each other through the radiation relations which are given for the various kinds of FELs in Table 1. In comparing various types of FELs and examining the dependence of their gain on the operating parameters, one should specify which are the independent parameters. In Table 3 the independent parameters are assumed to be λ, v_o and γ. The period L (or in the Cerenkov FEL - the index n) should be determined from the relations of Table 1.

The factor $1/2\ A_e \sqrt{\varepsilon_o/\mu_o}\ |\hat{\mathcal{E}}_z(x_e, y_e)|^2/P$ which appears in the first three rows of Table 1 can be interpreted as a generalized "filling factor" which indicates what fraction of the electromagnetic wave power participates in the interaction. In Table 3 row 3 the calculated expression for the filling factor of the electrostatic bremsstrahlung FEL [11] was substituted in. Numerical calculation of

this factor for Cerenkov FEL was given in [21]. In the case of a Smith Purcell laser structure, the calculation of the filling factor requires the full Floquet mode solution of the electromagnetic wave in the periodic waveguide. While such involved calculation would be avoided in the present work, it is important to point out that the filling factors of the Cerenkov and Smith-Purcell FELs are only a function of the waveguide and electron beam geometrical dimensions normalized to the radiation wavelength. Therefore if one scales the geometry of the waveguide and the beam in proportion to the operation wavelength, then it appears from the radiation conditions of Table 1, that over a wide range of wavelengths the filling factor is only a function of the independent parameters v_o and ζ, and does not depend directly on the wavelength λ. Consequently Table 3 is an explicit representation of the gain dependence on λ for the various FELs, assuming that the limiting factor is the current density J_o and that the waveguide geometrical dimensions of the laser amplifier are optimized for the operating wavelength. It is instructive to note that the wavelength dependence of the gain parameter $\bar{Q}$ is a proportionality relation for all FELs except the Cerenkov-Smith-Purcell type for which it is an inverse proportion.

The dependence of the gain parameter on the electron beam energy is not explicit in Table 3 for the Cerenkow-Smith-Purcell FELs, since the filling factors are a function of the electron velocity. However, it is probably correct to conclude that the gain parameter Q goes down as the energy is increased in all kinds of FELs, but in the longitudinal interaction FELs (first three rows in Table 3) it drops at a faster rate than in the transverse interaction FELs (last three rows).

In comparing magnetic and electrostatic bremsstrahlung FELs it is necessary to point out the basic advantage of the first kind which stems from the fact that the force applied on a relativistic electron by a magnetic field is usually much greater than the force applied by an electrostatic field considering the state of the art of laboratory available periodic magnetic and electric fields. However, if one considers free electron lasers also in the non relativistic regime, the magnetic force reduces by a factor β_{oz} leading to the β_{oz}^2 reduction factor in the gain parameter of the magnetic bremsstrahlung FEL as compared to the electrostatic bremsstrahlung FELs.

As a last point in the comparative discussion of free electron lasers gain we should indicate the advantage of transverse interaction FELs compared to the longitudinal interaction FELs in the consideration of waveguide losses of the electromagnetic wave. The effect of waveguide losses were not included in the present model. However, for practical FEL design it may be in some cases an important consideration, which cannot be ignored. To a good approximation it may be argued that the net gain of a free electron laser is equal to the gain of a lossless FEL structure substracted by the waveguide losses of the electromagnetic mode. Since transverse electric or transverse electromagnetic modes which are used in transverse interaction FELs suffer usually less waveguide losses than the transverse magnetic modes used in longitudinal interaction FELs, this provides a substantial advantage to the first kind when net gain is being compared.

6. FREE ELECTRON LASER EFFICIENCY

As discussed in a number of articles [32,33,37] high efficiencies of the order of tens of percents are potentially achieveable in free electron lasers using various efficiency enhancement techniques like tapering the pump period and intensity, or using energy retrieval schemes like storage ring or depressed collector (which is currently used in conventional traveling wave tubes). In this section we will consider only the basic efficiency η_o of the various FELs, noting, though, that this efficiency may be increased appreciably when efficiency enhancement techniques are used.

Since the efficiency of radiative energy extraction from the electron beam is limited by saturation effects, a full non linear analysis is necessary to derive the FEL efficiency η_o. Nevertheless it is possible to estimate its value from the linear analysis, by using a simple consideration presented by Sprangle et al[10]. For a magnetic bremsstrahlung FEL with a cold beam, this estimate has been shown to be in excellent agreement with the more rigorous self consistent nonlinear formulation of Ref.[32]. Also it agrees in the low gain regime with the results of Ref.[38] which was obtained with a much more elaborate analysis.

Consider any kind of FEL operating at any of the cold beam gain regimes discussed before (the warm beam regime must be discussed separately). The combined excitation of the coupled electromagnetic wave and the electron beam space charge waves has a component which propogates with wavenumber $k_{zo} = k_o + \mathrm{Re}\,k$ and phase velocity

$$v_{ph} = \frac{\omega}{k_{zo} + k_o + Re\,\kappa} \tag{86}$$

The estimate of FEL efficiency is based on the argument that the saturation mechanism is electron trapping in the periodic potential of the excitation, which propagates with phase velocity v_{ph} (86). It can be shown that the maximum deceleration in the electron velocity during the interaction up to full trapping is $2\,\Delta v_z$, where Δv_z is the initial axial velocity difference between the electron beam and the phase velocity of the trapping potential:

$$\Delta v_z = v_{oz} - v_{ph} = \frac{Re\,\kappa}{k_{zo}} + \left(\frac{\omega_p}{\omega}\right)^2 \frac{k_o}{\gamma_{oz}^2} c \tag{87}$$

Thus the maximum radiative energy extraction efficiency can be calculated as the relative change in the electron beam kinetic energy when its axial velocity decreases by Δv_z

$$\eta_o = \frac{\Delta\gamma_o}{\gamma_o - 1} = \frac{1}{\gamma_o - 1}\left(\frac{k_o}{v_{oz}}\right) 2\Delta v_z = \frac{\gamma_{oz}^2}{\gamma_o}\left(\frac{\omega_p}{\omega}\right)^2 \left(1 + \frac{k_o}{k_{zo}}\right)^{-1} \left(\frac{k_o}{k_{zo}}\right)$$

$$\left[\eta_o = \frac{1}{\gamma_{oz}^2}\left(\frac{\omega_p}{\omega}\right)^2 \frac{\lambda}{\pi}\right] \tag{88}$$

where

$$\tilde{\eta} \equiv \mathrm{Re}\hat{\delta}k - \hat{\delta} \qquad (89)$$

The expression in brackets corresponds to the highly relativistic limit.

The efficiency can now be calculated for any of the cold beam gain regimes described in section 4 by simply substituting the appropriate $\hat{\delta}$ and $\mathrm{Re}\hat{\delta}k$ in (88,89). These values of these parameters will be usually assumed to correspond to the maximum initial gain condition. The efficiency coefficient $\tilde{\eta}$ is in the case of a cold beam exactly the wavenumber mismatch drawn for various gain regimes in diagrams (b) to (e) of Fig. 4. It is listed in Table 4 for the different gain regimes. Notice that in the low gain and collective gain regimes $|\mathrm{Re}\hat{\delta}k| \ll |\hat{\delta}|$ and $\tilde{\eta} \simeq -\hat{\delta}$ and in the high gain strong coupling regime $|\mathrm{Re}\hat{\delta}k| \gg |\hat{\delta}|$ and $\tilde{\eta} \simeq \mathrm{Re}\hat{\delta}k$.

TABLE 4: The efficiency coefficent $\tilde{\eta}$ used for calculating the efficiency (88) at different gain regimes.

Gain regime	$\tilde{\eta}$
Low gain tenuous beam	$2.6/3$
Collective (low or high gain)	$\hat{\delta}_p$
High gain strong coupling	$\frac{1}{2}\,Q = \frac{1}{2}(\kappa\hat{\delta}_p^2)^{1/3}$
Warm beam high gain	$\frac{3}{5}[g'(\hat{\delta}_p)]^4 \frac{Q^3}{}_{th} = (=0.03)\frac{Q^3}{}_{th}$
Warm beam low gain	$g'(\hat{\delta}_p)\frac{1}{2}\,{}_{th} = (=1.)\frac{}{}_{th}$

The estimate of the laser efficiency in the warm beam high and low gain limits requires a somewhat different consideration. As is indicated from Eqs. (75) and (83), in these gain regimes only a small fraction of the electrons in the electron beam distribution participate in the interaction. In the high gain case these are the electrons with normalized axial velocities which lie in the regime $(\omega/v_z - k_r) \lesssim k_i = k_i v'_{zth}$, or that their velocities lie within the spectral width of the wave due to its growth $(\omega/v_z - k_r) \lesssim k_i$. From either of these relations we find that the class of electron velocities, which takes place in the interaction is:

$$v_z - v_{ph} \lesssim v_z - v_{ph} \frac{k_i}{k_r} \approx \frac{\delta k_i}{k_{zo}+k_o} \approx \frac{\delta k_i}{k_{zo}+k_o} \approx v_{oz} \frac{k_i}{k_{zo}+k_o} \qquad (90)$$

During the interaction the trapped electrons reverse their velocity relative to the phase velocity of the potential wave v_{ph}, until at saturation a local plateau is generated and $\bar{g}' \left(\frac{v_{ph} - v_{oz}}{v'_{zth}}\right) = 0$ (see Fig. 7).

In the warm beam low gain case the saturation process is similar, except that the class of electrons which participate in the interaction, is determined by the width of the spectral line shape function $\sin^2(\bar{\theta}'/2)/(\bar{\theta}'/2)^2$ which appears in the convolution (83):

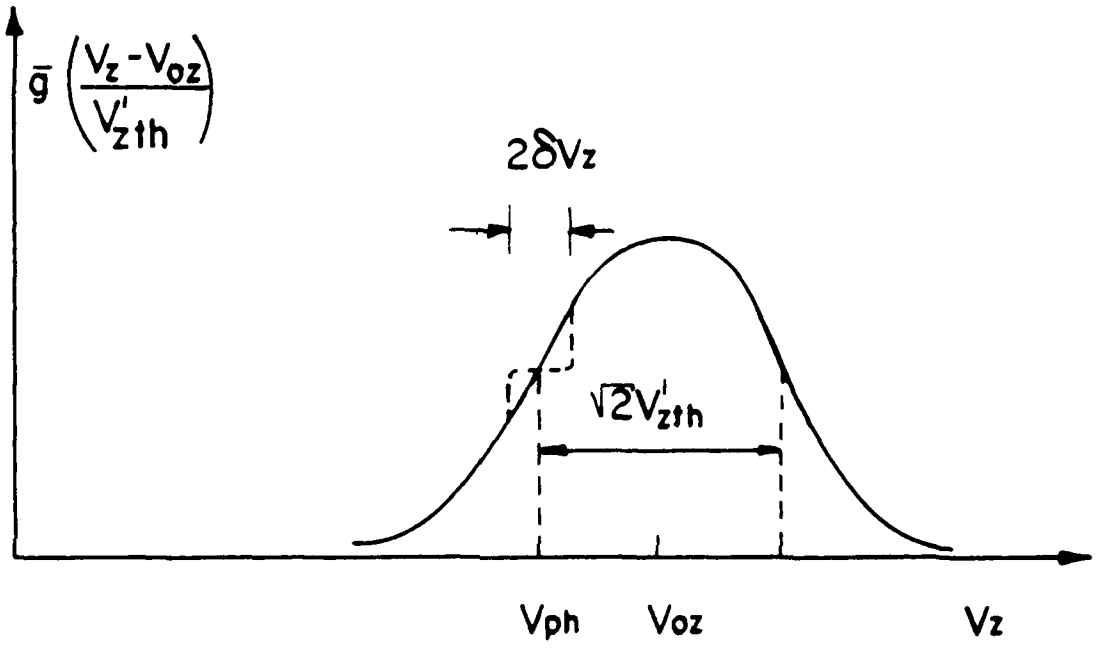

Fig. 7: The electron distribution function in the warm beam gain regime drawn in velocity space before (continuous line) and after saturation (broken line).

$|\bar{\delta}' - \bar{\delta}| = |\omega/v_z - v_{ph}| \lesssim$. The wave numbers of these electrons lie within the spectral width due to finite interaction length:

$|\frac{\omega}{v_z} - v_{ph}| \lesssim \pi/\ell$. These relations can be written as

$$|v_z - v_{ph}| \lesssim \Delta v_z = v_{oz} \frac{\bar{\quad}}{k_{zo}+k_o} \tag{91}$$

The radiation extraction efficiency of the free electron laser in the warm beam regimes is equal to the relative change in the kinetic energy due to the interaction, where the calculation of the change in beam kinetic energy before the interaction and after saturation is most conveniently done in momentum space:

$$\eta_o = \frac{\Delta E_{KE}}{E_{KE}} = \frac{1}{\gamma_o - 1} \frac{1}{n_o} \int_{p_{zph}-\delta p_z}^{p_{zph}+\delta p_z} (\gamma - 1)[g^{(o)}(p_z) - g^{(o)}(p_{zph})]dp_z \qquad (92)$$

where $p_{zph} = \gamma_{ph} m v_{ph}$ and $\delta p_z = \gamma_o \gamma_{oz}^2 m \delta v_z$. First order expansion of both γ and $g^{(o)}(p_z)$ around $p_z = p_{zph}$ and some mathematical steps give

$$\eta_o = \frac{1}{\gamma_o - 1} \frac{d\gamma_o}{dp_{zo}} \frac{dg^{(o)}}{dp_z}\bigg|_{p_{zph}} \frac{2(\delta p_z)^3}{3} = \frac{2}{3} \frac{\gamma_o \gamma_{oz}^2 \xi_{oz}}{\gamma_o - 1} g'(\zeta_r) \frac{(\delta v_z)^3}{c v_{zth}^3} \qquad (93)$$

Using (90), (91) and (77) we finally find that in both high and low-warm beam regimes the efficiency is given again by (88) with the parameter $\tilde{\eta}$ listed in Table 4 rows 4 and 5 for the high and low beam limits respectively. The expressions in parenteses were calculated for an electron beam with a Maxwellian distribution (33), assuming initial tuning to the maximum gain point $\zeta_r = -1/\sqrt{2}$.

The radiation extraction efficiency for <u>all FELs</u> and <u>all gain regimes</u> is estimated by the simple expression (88) with the efficiency coefficient $\tilde{\eta}$ given in Table 4 for the different gain regimes. *This expression applies* to FEL amplifier structures assuming saturation is reached within the interaction length ℓ. For oscilator structures (in which saturation is always obtained within the interaction length) it applies with the assumption of single mode operation (in particular for the warm beam case).

The efficiency depends on the interaction length ℓ only in the low gain-tenuous beam regimes (both cold and warm beam). Notice though that the expressions in Table 4 rows 1 and 3 apply with the assumption that saturation is reached right at the interaction length ℓ. In the cold beam low gain and collective regimes (rows 1, 2 in Table 4), the efficiency is proportional to λ and depends only on the beam parameters (velocity and density) and the interaction length. It is thus the same for all FELs considered. Also in the warm beam low gain regime (Table 4 row 3) the efficiency is independent on the kind of FEL considered and depends only on the parameters of the beam and the interaction length. The efficiency in this limit is proportional to λ^3.

In the high gain-strong coupling and high gain-warm beam limits (rows 3, 4 in Table 4) the efficiency depends on the kind of FEL considered through the parameter Q. Its dependence on wavelength and beam velocity varies for different FELs and can be found by substituting in (88) the corresponding $\tilde{\eta}$ parameter, the parameter θ_{th} (49) and the values of the parameter Q as listed in Table 4 for the different FELs. In all cases the efficiency η_o grows with the wavelength λ. This dependence is particularly strong in the high gain warm beam case, where it goes like λ^6 in the Cerenkov-Smith-Purcell FELs and λ^{12} in the bremsstrahlung FELs.

In the case when beam energy retrieval schemes are used the total efficiency can be calculated from the expression for the basic efficiency (88) by multiplying it by an efficiency enhancement factor M. This factor is equal in the case of a storage ring to the number of times that the electron beam can be recycled before its spread becomes intolerable, and in the case of a depressed collector scheme it is equal to the ratio between the electron beam

acceleration and collection voltages. In the case of efficiency enhancement by pump tappering we cannot use at all the estimate (88) and a full nonlinear analysis is necessary[32,33]

In conclusion of this section we will briefly discuss the revelations of the different saturation characteristics in the two seperately treated limits of warm and cold beams. We saw that while in the warm beam case only a class of electrons (90) or (91) participates in the interaction and gets trapped at saturation, in the cold beam limit all the electrons participate in the interaction and trapping process. As pointed out before in [17,39], the local plateau formation (Fig. 6) is analogous to the saturation and diminishing of population irversion in a class of atoms in Doppler broadened gas lasers. In terms of laser theory, the saturation nature of a warm beam FEL corresponds to inhomogeneous broadening and that of a cold beam to homogeneous broadening[40]

As in gas lasers there is "hole burning" effect in the gain curve of the warm beam FEL. However, there is still an important difference between the two: in contrast to the homogeneously broadened gas laser, the interaction mechanizm itslef changes the population of velocity classes in the vicinity of the interacting class of electrons. The gain curve of the saturated FEL (the derivative of the saturated distribution curve in Fig. 6) displays from the point of saturation on an effect of "hole burning" at $v_z \simeq v_{ph}$. But it also shows a new effect of "hill heaping" at the sides of the "hole" ($v_z \simeq v_{ph} \pm \Delta v_z$).

These different saturation behaviours will have explicit expression in FEL oscilation characteristics. In the homogeneous broadening-cold beam regime there will be "mode competition" between the modes of a long cavity laser, all "attempting" to extract power from the same electrons. This will tend to depress multimode operation in the laser. In the inhomogeneous broadening-warm beam regime, there will be at saturation an interesting new

effect of "mode cooperation" which will tend to increase the number of oscilating modes in a laser cavity which has a sufficiently dense spectrum of modes. The effect of "mode cooperation" will tend to wash out any bumps on the electron distribution function and spread it out, and will produce wide band radiation. Notice that this saturation ebhaviour is different from that of inhomogeneously broadened gas lasers, where there is no cooperation between the modes and there is even slight competition between close modes.

7. FREE ELECTRON LASER POWER

One of the most attractive qualities of free electron lasers seems to be the potential capability of high power operation. Since the interaction is done in vacuum and the active medium is not a material, problems of material damage and thermal distortion of the wave front are avoided. Since the radiation extraction efficiency of FELs can be made quite high, the laser power can be quite high too, and limited essentially by the electron beam power which can be drawn into the interaction region.

The radiative power which is generated by the free electron laser is

$$\Delta P = VI\eta_o \tag{94}$$

where η_o is the basic radiation extraction efficiency (88), I is the total beam current and V is the beam acceleration voltage

$$V = (\gamma_o - 1)\, mc^2/e \tag{95}$$

For a given efficiency and beam acceleration energy the radiative power generation (94) will depend only on the amount of electron current I which can be made to interact with the electromagnetic wave in the free electron laser. In many circumstances there will be a limit on the current density J_o which can be generated at the FEL input and propagated along the interaction length, hence the elimiting amount of interacting current will be given by

$$I = A_e J_o \tag{96}$$

Can the electron beam cross section A_e be increased indefinitely? Appart from various technical limitations we should be aware that the transverse dimensions of the electron beam should be limited by the range over which the periodic static fields and the electromagnetic mode field have an appreciable value, so that appreciable coupling coefficient (Table 2) exists to carry out the interaction. This limitation stems from the fact that the static periodic fields and the electromagnetic modes should satisfy the Laplace equation

$$(\nabla^2 \{ \underline{E}_o(x,y) \sin k_o z;\ \underline{B}_o(x,y) \sin k_o z \} = 0 \tag{97}$$

in the case of bremsstrhlung FELs, and the wave equation

$$(\nabla^2 + \frac{\omega^2}{c^2}) \{ \underline{\mathcal{E}}_1 (x,y) e^{i(k_{zo}+k_o)z} \} = 0 \tag{98}$$

for the Cerenkov-Smith-Purcell type (in the Cerenkov case $k_o = 0, \mathcal{E} \to \mathcal{E}_o$)

The solution of Eqs. 97, 98 in the case of a planar waveguide structure (Fig. 8a) is straightforward, giving for the bremsstrahlung FELs

$$E_o(x,y);\ B_o(x,y) \propto e^{-qx} \tag{99}$$

where

$$q = k_o = \frac{2\pi}{L} \tag{100}$$

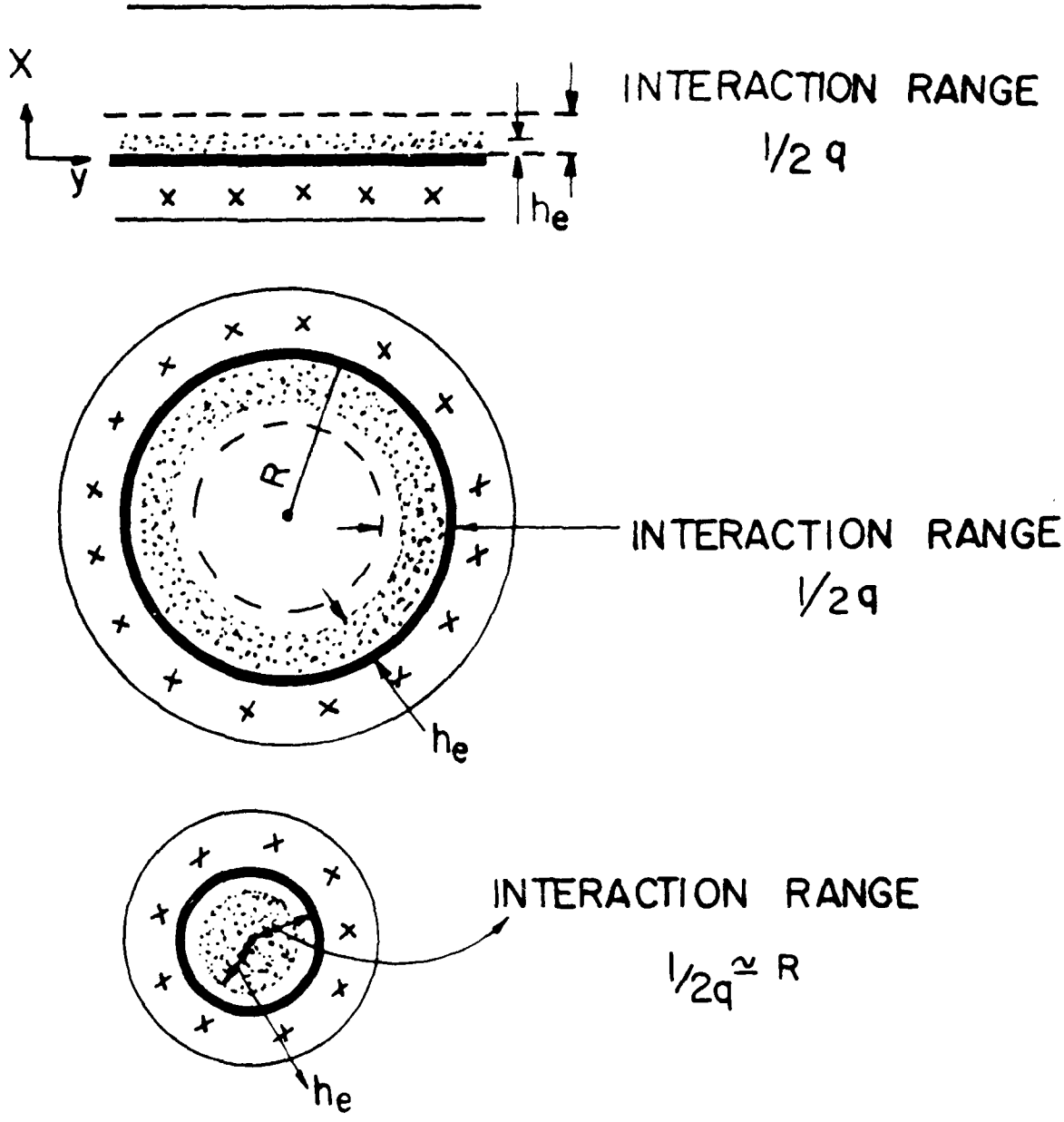

Fig. 8: Cross section diagrams of various FEL structures:

(a) Sheet beam in a planar waveguide structure.

(b) Annular beam in a cylindrical waveguide structure.

(c) Solid beam in a cylindrical waveguide structure.

The cross marked regions symbolize the source of periodic static field in bremsstrahlung FELs and the slow wave structure in Cerenkov-Smith-Purcell FELs.

and for the Cerenkov-Smith-Purcell FELs

$$\mathcal{E}_1(x,y) \propto e^{-qx} \tag{101}$$

where

$$q = \left[(k_{zo}+k_o)^2 - \frac{\omega^2}{c^2} \right]^{1/2} \tag{102}$$

Thus both the static pump field in the case of bremsstrahlung FELs and the slow electromagnetic wave component in the Cerenkov-Smith-Purcell FELs decay exponentially away from the source of periodic static field (magnets, coils or electrodes) or from the slow wave structure (periodic waveguide, dielectric waveguide). In order to obtain appreciable coupling coefficient (κ), the electron beam should be passed roughly within the range of one exponential e-folding distance of the squared field intensity: $1/(2q)$. This distance which we will term "the interaction range" can be found in terms of λ, β_{oz} and ϕ by substituting in (100,102) the synchronizm condition (4) and the radiation conditions of Table 1. The interaction range for the various FELs are listed in the second column of Table 5. The expressions in brakets correspond to the special case of $(\gamma_o >> 1)$ where for the longitudinal bremsstrahlung case we substitute in this limit $\zeta = \phi = (\sqrt{3}\gamma_o)^{-1}$

TABLE 5: Interaction range and maximum power of FELs

FEL	Interaction rage $\frac{1}{2q}$ / $(\frac{\lambda}{4\pi})$	Max. Power $\pm P_m$ / $(\frac{1}{4\pi^2}\frac{mc^2}{e} J_o w_e \tilde{\eta} \lambda^2)$
Trans. Brem.	$\frac{\beta_{oz}}{1-\beta_{oz}} = (1+\beta_{oz})\beta_{oz}\gamma_{oz}^2$ $[2\gamma_{oz}^2]$	$(1+\beta_{oz})\beta_{oz}^4\gamma_{oz}^4\gamma_o$ $[2\gamma_o\gamma_{oz}^4]$
Long. Brem.	$\frac{\beta_o}{1-\beta_o\cos\phi}$ $[\frac{3}{2}\gamma_o^2]$	$\frac{\beta_o^4\gamma_o^3}{1-\beta_o\cos\phi}$ $[\frac{3}{2}\gamma_o^5]$
Cerenkov - S.P.	$\beta_o\gamma_o$ $[\gamma_o^2]$	$\beta_o^4\gamma_o^4$ $[\gamma_o^4]$

In all FELs the interaction range $\frac{1}{2q}$ is proportional to the wavelength λ and only when the beam is highly relativistic ($\gamma_o >>1$) the interaction range can be appreciably larger than a wavelength. This explains why at short wavelengths it was necessary in recent FEL research to go to relativistic electron beams in order to obtain appreciable radiation. We see from Table 5 that in the highly relativistic limit, bremsstrahlung FELs have an advantage of roughly a factor γ_o in the interaction width compared to Cerenkov-Smith-Purcell FELs. There is no difference between them in the nonrelativistic limit ($\beta_{oz}<<1$).

For other waveguide cross section geometries like a cylindrical waveguide (Fig. 5b,c) the solution of (97,98) gives other function solutions for the transverse variation of the fields instead of (99, 101). For the case of a cylindrical waveguide the fields depend on the transverse coordinates like modified Bessel functions of the argument qr (r - the distance from the cylinder axis). When $r \gg 1/q$ the modified Bessel functions behave near the waveguide walls like exponential functions $\sim e^{qr}$. In a crude approximation we may extend the notion of interaction range to waveguides with general cross sections and claim that the interaction region, at which the coupling coefficient κ has an appreciable value, extends along the perifery of the waveguide within one interaction range $\frac{1}{2q}$ away from the walls (see Fig. 8 a, b). Out of this region the coupling coefficient drops down exponentially.

It is evident that for obtaining strong interaction it is usually preferable to pass the electron beam within the interaction region, where κ has its maximum value. So in the case of a planar geometry (Fig. 8a) we will prefer to use a sheet beam of dimensions $w_e \times h_e$ where w_e is the waveguide width and $h_e \approx 1/(2q)$. In the case of a cylindrical waveguide it is best to use an annular beam of thickness $h_e \approx 1/(2q)$ and perifery $w_e = 2\pi R$ (Fig. 8b). In case that the experimental conditions require the use of a solid cylindrical beam it is preferable (for the sake of obtaining appreciable gain) to keep the waveguide radius not much bigger than $R \approx 1/(2q)$. The beam cross section is then approximately $A_e = \pi (2q)^{-2}$.

It should be pointed out that at present, a detailed theoretical analysis of free electron laser interaction in the case where the fields vary transversely across the beam cross section is not available (except for

the thin beam approximation used here). In addition technical limitations may make it difficult in some cases to keep the electron beam within the interaction region, right next to the waveguide walls. Nevertheless, it is generally true that in either case the electron beam cross section area cannot be made much larger than the interaction region area if appreciable gain is to be attained, hence for the goal of estimating the upper bound of radiative power generation in free electron lasers the estimate that the useful electron beam cross section area is equal to the interaction region area:

$$A_e \approx w_e \times l/(2q) \tag{103}$$

is an appropriate approximation.

Using (95) (96) and (103) in (94), we get the expression for the maximum available power

$$\Delta P_m = \frac{1}{4\pi^2} \frac{mc^2}{e} J_o w_e \beta_{oz}^3 \gamma_{oz}^2 \gamma_o \left(\frac{l/2q}{\lambda/4\pi}\right) \bar{\eta} \lambda^2 \tag{104}$$

This is listed in the third column of Table 5 for the different kinds of FELs. The efficiency coefficient $\bar{\eta}$ is listed in Table 4 for the different gain regimes. The expressions in brakets in Table 5 correspond to the highly relativistic limit ($\gamma_o \gg 1$), where in the case of longitutinal electrostatic bremstrahlung FEL, operation at the maximum radiation angle $\theta_m = (\sqrt{3}\gamma_o)^{-1}$ was assumed.

The stimulated Compton-Roman scattering is not included in Table 5, because in this special case there is no limit on the interaction region width and it is simply determined by the electron beam width (assuming it is narrower than the pump electromagnetic wave). The maximum power in this case (in the highly relativistic limit) is given by

$$[CP_m = \frac{1}{\cdot} \frac{mc^2}{e} J_o A_e {}^{1}{}^{2}_{oz} \gamma_o \tilde{\eta} \cdot \cdot] \tag{105}$$

The lack of interaction width limitation in the case of the Compton-Raman FEL is a very important advantage of this FEL kind in the limits of short wavelengths and moderate beam energy. Thus a viable option for producing radiation in this limit may be the composition of a two step FEL, in which one kind of FEL produces high power radiation at a relatively long wavelength, and this radiation operates as a pump in an adjacent Compton-Raman laser which produces radiation at a short wavelength. Simultaneous operation of a bremsstrahlung and a Compton-Raman FELs, operating as spontaenous emission amplifiers, was demonstrated in Ref. [41].

In the cold beam low gain regime (which may be in particular a useful operation regime in FEL oscilators) and in the collective regime ($\tilde{\eta} = 2.6/\ell$ and $\tilde{\eta} = \theta_p$ respectively) the maximum power is proportional to λ^2 for all FELs, and to λ for Compton-Raman scattering. In both cases it is independent on the FEL gain parameter (or coupling coefficient). Nevertheless it cannot be concluded that laser gain is inmaterial in determining the laser power. It should be recalled that the assumption is in all cases that the laser saturates within

the interaction length ℓ. In the case of a very low gain laser this assumption would require an impracticable input power (in the case of amplifier) or impracticable resonater quality (in the case of a laser oscilator). Thus, even in the low gain regime the laser gain will indirectly affect the maximum available power through the choice of ℓ.

In the warm beam low gain regime the substitution of $\bar{\ell}_{th}$ (49) and $\bar{r}$ (Table 4 row 5) results in (104) a λ^{5} wavelength dependence of the maximum power available in all FELs except Compton-Raman FEL (105) for which there is a λ^{4} dependence.

In the high gain strong coupling and warm beam regimes there is an explicit dependence of the maximum power on the gain parameter Q. From Tables 3,4,5 we find that the maximum power generation of all FELs still grows with λ for all FELs considered. There is a particularly strong wavelength dependence in the high gain warm beam case. This dependence goes like λ^{7} in the Cerenkov-Smith Purcell FELs, like λ^{13} in the bremsstrahlung FELs, and like λ^{12} in the Compton-Raman FEL.

It is instructive to point out that the maximum power generation grows very strongly with beam energy in all FELs and all cold beam regimes. We may say that appart from the possibility of generating short wavelength at high electron beam energies, the high power generation level at this limit is what distincts most markedly modern free electron lasers development from classical microwave tubes.

We see from Table 5, Column 3, that in the highly relativistic limit bremsstrahlung FELs have an advantage in maximum power generation by a factor of about γ_0 compared to the Cerenkov-Smith-Purcell FELs, (at least in the low gain and collective regimes). This stems from the fact that the interaction width of the first kind is larger from that of the second

kind by the same factor (Table 5 column 2). In the nonrelativistic limit ($\beta_o << 1$) the maximum power generation drops down in these regimes at the same fast rate (like β_o^4) for both kinds of FELs.

We point out that the expression of maximum power generation derived in this section applies without change also for FELs with energy retrieval schemes, but of course fails completely in efficiency enhancement schemes like tapering. However, if the total efficiency η in the latter case is known, the maximum power ΔP_m can be still calculated from Eqs. 94, 95, 96 and 103 with η_o substituted by η and $1/(2q)$ given in Table 5.

In practice various technical limitations will not allow passing the electron beam too close to the magnetic coil, grating etc. and the optimal case where the whole interaction range cross section is filled with electrons (103) cannot be materialized. In this case the practically extractable power falls short of the maximum extractable power by a factor $I_o/(J_o w_e 1/2 g)$ which is the ratio between the actual current I_o and the maximum current which would ideally be passed through the interaction region cross section.

As an example consider a case of a transverse bremsstrahlung FEL operating in the cold beam low gain regime with parameters values similar to those of the Stanford experiment[49]: $\gamma_o = 48$, $\gamma_{oz} = 39$ ($B_o = 0.24$ Tesla), $n_o = 2 \times 10^9 cm^{-3}$ ($J_o = 9.6$ A/cm^2), $\lambda = 10.6 \mu$ m and $L = 5.2$m. We assume in this example that a solid cylindrical beam is used and therefore substitute in (104) $w_e = \pi x 1/(2q)$ where $1/(2q)$ is given in Table 5 row 1 and x in Table 4 row 1. Hence the maximum extractable power in such a case is given by

$$\Delta P_m = \frac{2.6}{4\pi^2} \frac{mc^2}{e} J_o \gamma_{oz}^6 \gamma_o^{-3} \qquad (106)$$

which gives ΔP_m = 84 KW. In the actual experiment the need to insulate the superconducting magnet did not allow the use of an optimal size beam which fills the whole interaction region $J_o \times \pi(1/2q)^2 = 2A$ (as assumed in (106) and only a current of 70 mA was passed in the center of the waveguide. Hence the expected (and indeed also the measured power generation falls short from the calculated maximum power generation in proportion to the current ($\Delta P \simeq 84 \times 0.07/2 \simeq 3$ KW).

8. Free Electron Laser Spectral Width

In all gain regimes considered in section 4 the gain is a function of the detuning parameter $\delta = \frac{\omega}{v_{oz}} - k_{zo} - k_o$ (43). In each gain regime there is an optimal value of the detuning parameter δ_m (which is always negative), for which the gain is maximal. The values of δ_m at the different gain regimes are given in Table 6. The phase matching diagrams corresponding to the maximum gain condition are drawn in Fig. 4 for the different gain regimes.

When we keep all the laser Operating Parameters constant and only change the radiation wavelength λ, the detuning parameter δ changes from its maximum gain value δ_m. The differentiation of (43) gives

$$\Delta\omega = \frac{\Delta\delta}{v_{oz}^{-1} - v_g^{-1}} \tag{107}$$

where

$$v_g = \frac{d\omega}{dk_z} \tag{108}$$

is the group velocity of the electromagnetic mode in the waveguide.

Eq. (107) applies to all FELs. In Cerenkov FEL the evaluation of the group velocity of the mode v_g may require the complete solution of the uncoupled mode dispersion relation in the dielectric waveguide. The group velocity in this case may depend on the index of refraction dispersion of the dielectric $dn/d\omega$ as well as the waveguide dispersion. In all other FEL

structures the group velocity can be evaluated straightforwardly if we assume that ϕ (in Eq. 5) is a weak function of the wavelength. This is true in modes of waveguides with wide cross section, and particularly true in all the transverse FELs, in which $\phi = o$. In these cases

$$v_g = \frac{c}{\cos \phi} \tag{109}$$

and substitution in (107) gives

$$\frac{\Delta\lambda}{\lambda} = \frac{\Delta\theta}{k_{oz}^{-1} - \cos \phi} \tag{110}$$

or using the radiation conditions of Table 1.

$$\frac{\Delta\lambda}{\lambda} = \frac{\Delta\theta}{k_o} \tag{111}$$

If $\Delta\theta$ is the range of detuning parameter value around θ_m over which there is still gain, than $\Delta\omega$ or $\Delta\lambda$ are the laser spectral widths in the frequency or wavelength domain.

The parameter $\Delta\theta$ can be evaluated in the different gain regimes simple inspection of the gain dependence on θ (Eq. 78, Fig 6 in the warm beam limit, and Eq. 55, Fig. 5 in the low gain-cold beam limits) and by some algebraic investigation of the dispersion relation (41) in the cold beam-high gain regimes (collective and strong pump). The results are given

in Table 6. The wave number mismatch ranges, over which the laser has gain, are also illustrated in Fig. 4 for the various gain regimes.

Table 6: The detuning parameter value of maximum gain $\bar{\nu}_m$, and the detuning parameter range of gain $\Delta\bar{\nu}$.

Regime	$\bar{\nu}_m$	$\Delta\bar{\nu}$
Low gain-tenuous beam	$-2.6/\ell$	$2\pi/\ell$
Low gain-space charge	$-\bar{\nu}_p$	$2\pi/\ell$
High gain-collective	$-\bar{\nu}_p$	$2\sqrt{2\kappa\bar{\nu}_p}$
High gain-strong pump	0	$2Q^{1/3}$
Warm beam	$-\frac{1}{\sqrt{2}}\bar{\nu}_{th}$	$2\bar{\nu}_{th}$

For all FELs the spectral width is given by substituting the appropriate parameter $\Delta\bar{\nu}$ in Eqs. 110, 111 or 104 . Only in the high gain regime (rows 3,4, in Table 6) does the spectral width $\Delta\omega$ depend on the particular kind of laser or on the wavelength λ through the coupling parameter κ or the gain parameter Q which are given in Table 2 and 3 respectively.

From the validity conditions of the different gain regimes it comes out that the parameter $\Delta\bar{\nu}$, and consequently the spectral width, grow up the lower the gain regime is listed in Table 6. Hence the lower limit

on the spectral width occures in the low gain regimes (row 1,2). In Eq. 111 it gives

$$\frac{\Delta\lambda}{\lambda} = \frac{L}{\ell} \tag{112}$$

This is usually quite a wide spectral width, which grows with wavelength and beam velocity (as can be varified by substituting the radiation conditions from Tabel 1). In a typical example like the Stanford experiment [42]

$(L = 3.2\ \text{cm}\quad \ell = 5.2\ \text{m}),\ \frac{\Delta\lambda}{\lambda} = 0.6\%.$

References

1. H. Motz, J. Appl. Phys. 22, 527 (1951)

2. J.M. Madey, Appl. Phys. 42, 1906. (1971).

3. F.A. Hopf, P. Meystre, M.O. Scully and W.H. Louisell, Optics Commun. 18, 413 (1976).

4. N.M. Kroll and W.A.McMullin Phys. Rev. A17, 300 (1978).

5. W.B. Colson, Physics of Quantum Electronics Vol.5, p. 157 (Ed. S. Jacobs, M. Sargent III and M. Scully) Addison-Wesley Pub. (1978).

6. T. Kwan, J.M. Dawson and A.T. Lin, Phys. of Fluids 20, 581 (1977).

7. A. Hasegawa, Bell System Tech. J. 57, 3069 (1978).

8. A. Bambini, A. Renieri, S. Stenhalm, Phys. Rev. A, 19 2013 (1979).

9. I. Bernstein and J.L. Hirshfield, Phys. Rev. A - 20, 1661, (1979).

10. P. Sprangle, R. Smith and V.L. Granatstein, Infrared and Millimeter Waves Vol 1, p. 279 (Ed. K.J. Button) Academic Press (1979); see there more ref.

11. A. Gover, Physics of Quantum Electronics Vol.7 (Eds. S. Jacobs, M.Sargent III and M. Scully) Addison-Wesley Pub. (1980).

12. G. Bekefi and R.E. Shefer, 1979 IEEE International Conf. on Plasma Science, Montreal, Canada, Conf. Record p. 12, 13; G.Bekefi and R.E. Shefer J. Appl. Phys. 50, 5158 (1979).

13. R.H. Pantell, G. Soncini and H.E. Puthoff, IEEE J. Quantum Electronics 4, 905 (1968).

14. V.P. Sukhatme and P.W. Wolff, J. Appl. Phys. 44, 2331 (1973).

15. V.A. Dubrovskii, N.B. Lerner and B.G. Tsikin, Sov. J. Quant. Electron., 5, 1248 (1976).

16. P. Sprangle, A.T. Drobot, J. Appl. Phys. 50, 2652 (1979).

17. A. Gover, A. Yariv, Appl. Phys. 16, 121 (1978).

18. J.E. Walsh, T.C. Marshall, M.R. Mross and S.P. Schlesinger, IEEE Transac. MTT-25, 561 (1977); J.E. Walsh Physics of Quantum Electronics Vol.5 p. 357 (Eds. J. Jacobs, M. Sargent III and M. Scully) Addison Wesley Pub. (1978).

19. A. Yariv, C.C. Shih, Optics Commun. 24, 233 (1978).

20. A. Gover, Z. Livni, Optics Commun. 26, 375 (1978).

21. Z. Livni, A. Gover, Linear Analysis and Implementation Considerations of Free Electron Lasers Based on Cerenkov and Smith-Purcell Effects, Tel Aviv University, School of Engineering, Quantum Electronics Lab. Scientific Report 1979/81 (AFOSR 77-3445).

22. S.J. Smith, E.M. Purcell, Phys. Rev. 92, 1069 (1953).

23. F.S. Rusin, G.D. Bogomolov, Proc. of the IEEE, 57, 720 (1968).

24. V.K. Korneyenkov, V.P. Shestopalov, Radio Eng. Electr. Phys. 22, 148 (1977).

25. K. Mizuno, S. Ono, Y. Shibata, IEEE Transac. ED-20, 749 (1973).

26. R.M. Phillips, IRE Transac. ED-7, 231 (1960).

27. L.A. Vaynshtain, Electromagnetic Waves, Sovietskoye Radio, Moskow (1957) (Russian)

28. M.R. Mross, T.C. Marshall, P.E. Efthimion, S.P. Schlesinger, 2nd International Conf. on Submillimeter Waves, Puerto-Rico, Dec. 1976, Conf. Digest p. 128.

29. B.D. Fried, S.D. Conte, The Plasma Dispersion Function, Academic Press, New York (1971).

30. J.R. Pierce, Travelling Wave Tubes, Van Nostrand, Princeton (1950).

31. W.B. Louisell, J.F. Lam, D.A. Copeland, Phys. Rev. A 18, 655 (1978).

32. P. Sprangle, C. Tang, W.M. Manheimer Physics of Quantum Electronics Vol. 7 (Eds. S. Jacobs, M. Sargent III and M. Scully) Addison-Wesley Pub. (1980); ibid to be published in phys. Rev. Lett. (1980).

33. N.M. Kroll, Physics of Quantum Electronics Vol.7 (Eds. S. Jacobs, M. Sargent III and M. Scully) Addison-Wesley Pub. (1980).

34. P.S. Sprangle, V.L. Granatstein, L.Baker Phys. Rev. A-12, 1697 (1975).

35. D.B. McDermott, T.C. Marshall, Physics of Quantum Electronics. Vol. 7 (Eds. S. Jacobs, M. Sargent III and M. Scully) Addison-Wesley Pub. (1980).

36. D.B. McDermott, T.C. Marshall, S.P. Schlesinger, R.K. Parker, V.L. Granatstein, Phys. Rev. Lett. 41, 1368 (1978).

37. L.R. Elias, Phys. Rev. Lett. 42, 977 (1979

38. F. A. Hopf, M. Meystre, M.O. Scully, W.H. Louisell, Phys. Rev. Lett. 37, 1342 (1976).

39. F.A. Hopf, P. Meystre, G.T. Moore, M.O. Scully, Physics of Quantum Electronics Vol. 5, p.41 (Eds. J. Jacobs, M. Sargent III and M. Scully) Addison Wesley Pub. (1978).

40. A. Yariv, Quantum Electronics, John Wiley, New York (1975).

41. V.L. Granatstein, S.P. Schlesinger, M. Herndon, R.K. Parker, I.A. Pasour, Appl. Phys. Lett. 30, 384 (1977).

42. L. Elias, W. Fairbank, J. Madey, H.A. Schwettman, T. Smith, Phys. Rev. Lett. 33, 717 (1976).


DAT
FILM